



# D4.2

---

## REPORT ON 5G RADIO DEPLOYABILITY IN THE FACTORY

The 5G-SMART project has received funding from the European Union's Horizon 2020 research and innovation programme under grant agreement no 857008.



## D4.2 REPORT ON 5G RADIO DEPLOYABILITY IN THE FACTORY

Grant agreement number:	857008
Project title:	5G for Smart Manufacturing
Project acronym:	5G-SMART
Project website:	<a href="http://www.5gsmart.eu">www.5gsmart.eu</a>
Programme:	H2020-ICT-2018-3
Deliverable type:	Report (R)
Deliverable reference number:	D14
Contributing work packages:	WP4
Dissemination level:	Public (PU)
Due date:	31 <sup>st</sup> August 2020
Actual submission date:	31 <sup>st</sup> of May 2022 (M36)
Responsible organization:	ULUND
Editor(s):	Sara Gunnarsson (ULUND) Fredrik Tufvesson (ULUND)
Version number:	2.0
Status:	Final
Short abstract:	This deliverable presents results from the work carried out regarding the channel measurements and electromagnetic compatibility (EMC) tests that have been conducted in the Bosch semiconductor factory in Reutlingen. This includes details of the designed test setups, measurement scenarios and evaluation of both the channel measurements and EMC tests.
Keywords:	5G, ASIC, channel characterisation, massive multiple-input multiple-output (MIMO), measurements, mmWave, semiconductor test, sensor

Contributor(s):	Sara Gunnarsson (ULUND) Steffen Malkowsky (ULUND) Harsh Tataria (ULUND) Fredrik Tufvesson (ULUND) Joachim Schwarz (BOSCH) Uwe Glass (BOSCH) Horst Raidt (BOSCH) Ahmad Rostami (BOSCH)
-----------------	--



---

## Disclaimer

This work has been performed in the framework of the H2020 project 5G-SMART co-funded by the EU. This information reflects the consortium's view, but the consortium is not liable for any use that may be made of any of the information contained therein.

This deliverable has been submitted to the EU commission, but it has not been reviewed and it has not been accepted by the EU commission yet.



---

## Executive summary

As a part of the evaluation and deployment of 5G in real operating manufacturing factories, this deliverable presents two important aspects to consider, namely evaluation of coverage and electromagnetic compatibility (EMC). For this evaluation, two channel measurement setups, operating in two different bands have been considered together with setups to be able to conduct EMC tests. Measurements and tests have been performed at the Bosch semiconductor factory in Reutlingen, an environment where both coverage and EMC are important but challenging to achieve due to the complicated environment and high requirements.

The scenarios considered for the channel measurements are presented as well as the different types of devices that have been under evaluation in terms of EMC. Results are presented where, for the channel measurements, the possibilities and challenges with deploying a radio system in a factory are shown. The EMC evaluation, correspondingly, showcase the potentials and risks in terms of achieving EMC in this specific type of production.

To summarize this initial assessment, the results from the mid band channel measurements are promising for providing coverage across a factory floor. Unfortunately, issues were identified in the post-processing of the higher frequency measurements and hence, no results from these measurements can be presented. Regarding the EMC evaluation, depending on the requirements from the production, compatibility might not always be guaranteed. Further investigations are required for both aspects and in the end of this deliverable, ways forward will be presented.



## Table of content

Executive summary .....	1
Table of content.....	3
1 Introduction .....	5
1.1 Objective of the document .....	6
1.2 Relation to other documents .....	6
1.3 Structure of the document .....	6
2 Channel measurement systems.....	7
2.1 Mid band massive MIMO channel sounding system .....	7
2.2 Millimeter-wave channel sounding system .....	9
3 Channel measurement scenarios.....	11
3.1 Scenario A: open corridor .....	11
3.1.1 Mid band measurements.....	12
3.1.2 Millimeter-wave measurements.....	13
3.2 Scenario B: semi-open environment with robot interaction .....	13
3.2.1 Mid band measurements.....	14
3.2.2 Millimeter-wave measurements.....	15
3.3 Scenario C: heavy blockage.....	16
3.3.1 Mid band measurements.....	17
3.3.2 Millimeter-wave measurements.....	18
4 Channel characteristics .....	18
4.1 Mid band characteristics.....	19
4.1.1 Scenario A: open corridor .....	19
4.1.2 Scenario B: semi-open environment with robot interaction .....	21
4.1.3 Scenario C: heavy blockage.....	27
4.2 Millimeter-wave characteristics.....	46
4.2.1 Scenario A: open corridor .....	47
4.2.2 Scenario B: semi-open environment with robot interaction .....	48
4.2.3 Scenario C: heavy blockage.....	51
4.3 Summary of channel characteristics .....	55
5 Electromagnetic compatibility tests .....	56
6 Device selection .....	58



---

7	EMC test setup .....	59
7.1	Test sequence and procedure.....	61
7.2	Safety for series production.....	62
7.3	Analysis tool .....	62
8	EMC evaluation .....	63
9	Conclusions and ways forward .....	66
10	References .....	68
	Appendix .....	69
	List of abbreviations.....	69



## 1 Introduction

When deploying 5G systems in factory environments to be used for smart manufacturing, two essential aspects that need investigation are whether reliable coverage, to ensure that use case requirements are fulfilled across the factory floor, can be provided and if the electromagnetic compatibility (EMC) levels of 5G technology are satisfactory. To investigate this, 5G-SMART has as one of its objectives that the deployability of 5G system in a Bosch semiconductor factory environment should be evaluated in terms of these previously mentioned aspects. To evaluate the coverage in the production environment, channel measurements have been performed, taking into account various aspects that are obstacles to the radio propagation. Furthermore, a semiconductor production environment is sensitive to radiation and hence has high requirements on EMC levels and therefore a test setup has been designed and devices have been tested.

Since a factory floor is a challenging environment in terms of radio propagation, attention needs to be given to how to provide a reliable coverage throughout the factory. Factory floors are usually environments characterised as rich scattering with various tools and machines, which contribute to shadowing effects and are in different ways interacting with the radio signals. Moreover, the environment is typically quite dynamic as production is ongoing with people and robots moving around performing their tasks. To investigate the effects of these aspects, channel measurement campaigns have been designed to investigate power distributions at various positions across the factory floor, blocking profiles, behaviour and characteristics of multipath components (MPCs) and polarisation parameters. The measurements are designed to consider two 5G frequency bands, both a mid band frequency centred around 3.71 GHz and also a higher frequency centred around 27.5 GHz.

Another factor to consider is that the production could potentially be sensitive to environmental conditions, such as radio signals. As a result, it is crucial to make sure that 5G signals do not have any negative impact on the production processes before any 5G system is deployed and operated in the production area. To address this issue, the impact of 5G signals on a semiconductor production is analysed and evaluated. The focus is on the semiconductor testing process, which is an important process of the whole semiconductor production. In particular, the electromagnetic fields created due to the 5G signals are investigated to see whether these could have any negative impacts on the testing of the produced semiconductor components, i.e. EMC.

With the information that can be extracted from the two different types of investigations, valuable insights are provided regarding the feasibility of deploying 5G systems for smart manufacturing in real operating factories. Input is given regarding how to design the system from a radio propagation point of view as well as in terms of electromagnetic compliance. The results can also be used for further analysis and to design relevant models to be used for 5G deployment in factory environments.

The channel measurements and EMC tests have both been conducted in the Bosch semiconductor factory in Reutlingen as seen in Figure 1; the channel measurements were performed in the wafer fab, whereas the EMC tests were performed at the wafer test area and the final test area of the devices.





Figure 1. Overview of Bosch semiconductor factory in Reutlingen, Germany

## 1.1 Objective of the document

One of the overall objectives for 5G-SMART is to evaluate the possibility of deploying 5G in a semiconductor factory. One aspect is to evaluate this in terms of channel measurements and EMC tests. The objective of this document is to describe the measurements and tests made and to present the first results from these experiments.

## 1.2 Relation to other documents

This deliverable is related to the work presented in D1.1 [5GS20-D110] and D4.1 [5GS20-D410]. While the first one relates to the use cases to be trialed in the Bosch semiconductor factory, the latter describes the constraints and deployment requirements for the design and installation of the 5G system. In D4.1 [5GS20-D410] more details regarding the trial site are described and this document aims at adding to this document by presenting further insights related to 5G radio deployment in the factory.

## 1.3 Structure of the document

This deliverable is structured in two parts, the channel measurements and the EMC tests. First an overview of the equipment used for the channel measurements are given, followed by descriptions of the chosen measurement scenarios. Then the channel characterisation results are presented. For the EMC part, an introduction to the EMC tests is given and the motivation for the selection of devices used for the tests is presented. The test setup, both in terms of hardware and the test procedures applied, is described. Then the evaluation of the EMC test results is provided. Finally, conclusions and steps for how to proceed are outlined, both regarding the channel measurement results as well as the EMC test results.





## 2 Channel measurement systems

For the channel measurements, two systems were considered. One real-time massive multiple-input multiple-output (MIMO) testbed for the mid band measurements and one channel sounder with a switched array for the millimeter-wave (mmWave) measurements. Both of them will be further described below.

### 2.1 Mid band massive MIMO channel sounding system

The mid band channel sounding system is a software-defined radio (SDR) massive MIMO system with 100 radio-frequency (RF) chains. The so-called Lund university massive MIMO (LuMaMi) testbed, which is acting as a base station (BS) is shown in Figure 2. The testbed implementation is based on Long-Term Evolution (LTE) and is using orthogonal frequency-division multiplexing (OFDM). Each user equipment (UE) sends pilots on orthogonal subcarriers, i.e., each UE uses every 12-th subcarrier with the first UE starting at subcarrier 0, the second at subcarrier 1, etc. A summary of the testbed parameters can be found in Table 1 and further details about the testbed and sounding system can be found in [MVL+2017].

The planar T-shaped antenna array with 160 dual polarised  $\lambda/2$  patch elements was developed in-house. A 3.2 mm Diclad 880 was chosen for the printed circuit board substrate. The 160 dual-polarised antennas yield in total 320 possible antenna ports that can be used to explore different antenna array configurations. The default configuration is that the top four rows are connected to the 100 RF chains with alternating polarisation; the upper left antenna is vertically polarised, the next one it horizontally polarized and so on, creating an array where both polarisations are utilized, equally spaced and with similar aperture. All antenna elements are center shorted, which improves isolation and bandwidth. The manufactured array yielded an average 10 dB-bandwidth of 183 MHz centered at 3.7 GHz with isolation between antenna ports varying between 18 dB and 28 dB depending on location in the array. During the measurement campaign a distributed setup was also considered with 100 dipole antennas, each having a 5-meter cable. The setup, when mounted in the factory, can be seen in Figure 3. For this setup, the antennas were mounted at random places with random polarisations with the aim to exploit signals coming from all possible directions.

Each UE represents a phone or other wireless device with single antenna capabilities. One SDR serves as two independent UEs such that overall six SDRs are required when deploying all 12 UEs. Each UE is equipped with an omni-directional dipole antenna and both vertical and horizontal polarisations of the antenna can be achieved by physically rotating the antenna in the setup.



Figure 2: The Lund university massive MIMO (LuMaMi) testbed.

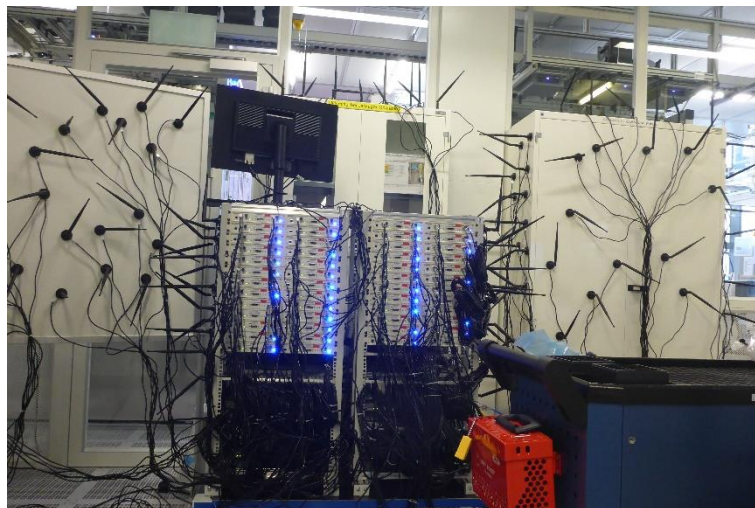


Figure 3: The distributed array mounted in the factory.

Table 1: Summary of the testbed parameters.

Parameter	Value
Sounder type	Real-time testbed
Center frequency	3.7 GHz
OFDM symbol duration	66.67 $\mu$ s



Snapshot rate	10 ms
Bandwidth	20 MHz
BS output power	16 dBm per antenna
BS array size	100 antennas
Antenna gain for patch antennas	8 dBi (simulated)
Polarisation	Dual - vertical and horizontal
BS-UE synchronization	Over the air
Number of UEs	Up to 12 simultaneously
UE transmit power	18.5 dBm
UE array size	1 antenna
UE antenna	Omni-directional dipole

## 2.2 Millimeter-wave channel sounding system

The general principle of the mmWave channel sounding system is as follows: a known waveform is generated in the baseband and up-converted to the carrier frequency of interest, followed by power amplification and transmission. On the receiving end, the waveform is down-converted, sampled and stored for post-processing. The channel impulse response is extracted from the received signal envelope relative to what was transmitted. In order to extract the directional characteristics of the channel, multiple repetitions of the sounding waveform are transmitted into, and hence received from, different directions, illuminating different transmit and/or receive antennas.

The baseband sounding waveform implemented at the transmitter's host interface is a multi-tone Zadoff-Chu (ZC) sequence. ZC sequences have ideal correlation properties in both time and frequency domains and are thus well suited for channel sounding. In contrast to other sounding waveforms, they are also easily scalable across both time and frequency domains. Naturally, wider signal bandwidths facilitate higher frequency selectivity, while the total duration of the sounding waveform is designed keeping in mind the furthest resolvable MPC.

The sounder, as seen in Figure 4, is designed with a 128 element uniform planar array at the transmitter, here acting as the BS, and a 256 element cylindrical array at the receiver, here being the UE, supporting dual polarisation. Both arrays are equipped with integrated RF switches to switch through each antenna combination from the transmitter to the receiver. According to the switched array principle, both link ends are equipped with a single RF up/down-conversion chain. Further details of the sounder setup can be found in [Ben19].

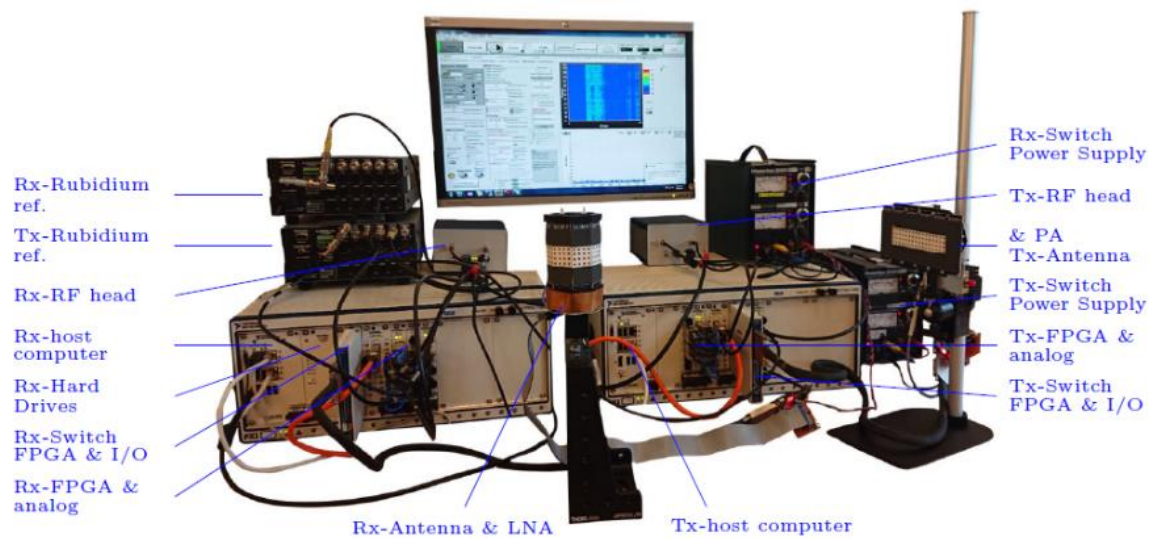


Figure 4: The mmWave equipment.

Each patch antenna is designed as a coupled parasitic resonator where the feed element is connected through stacked vias to the switch outputs at the antenna backplane. The elements are designed in a three-layered structure. The lowest layer is the ground plane, the second layer elevated to 100  $\mu\text{m}$  is a dual feed coupling element and the top layer at 300  $\mu\text{m}$ , is the radiator. The coupling element in combination with the radiator generates two closely spaced resonances that are tuned to achieve a bandwidth that covers the desired frequencies. Each antenna element is individually characterized in an anechoic chamber such that a high resolution parameter estimation algorithm can be used for estimation of the channel parameters. Further details of the antenna design can be found in [YZB+20]. Table 2 presents a summary of the parameters used for the mmWave channel measurements.

Table 2. Summary of the sounder parameters.

Parameter	Value
Sounder type	Switched array
Center frequency	27-28 GHz
Bandwidth	1 GHz
Transmit equivalent isotropically radiated power	32 dBm
BS array size	128 antennas
UE array size	256 antennas
Polarisation	Dual - vertical and horizontal
UE antenna gain	27 dB (after post processing)
Direction switching rate	10 $\mu\text{s}$
Snapshot rate	327.68 ms
BS-UE synchronization	Rubidium clocks



### 3 Channel measurement scenarios

For the channel measurements, three different main scenarios were considered. In this section, these scenarios are further described and the details of the measurement campaign will be presented. In short, the three scenarios are open corridor, semi-open environment with robot interaction and heavy blockage; the choice of the respective scenario is also elaborated on in this section. The specific experiments performed for the two frequency bands are also outlined. Due to practical constraints, the experiments for the two bands are not always exactly the same.

#### 3.1 Scenario A: open corridor

Scenario A includes a long corridor where there are walls and equipment constituting corridors on one side and a wall with glass windows leading to the next room with equipment on the other side. The environment is quite dynamic due to human interaction as people are walking along the corridor and crossing when moving between rooms or transporting equipment and products.

This scenario, as roughly shown in Figure 5, was chosen since it is considered a suitable reference scenario for industrial environments. The corridor is around 2 meters wide and goes through the whole factory. The part of the corridor shown in the figure is approximately 30 meters long. High metallic equipment as well as propagation effects caused by other materials characterize the environment; this can be seen in Figure 6. It is also a suitable scenario for performing reference measurements with a direct link (LOS link) as well as investigating the time evolution of the channel when increasing the distance between the BS and UE. It is also possible to investigate shadowing and blockage profiles when moving the user around a corner. Naturally, the human interaction is also expected to contribute to large-scale fading effects.

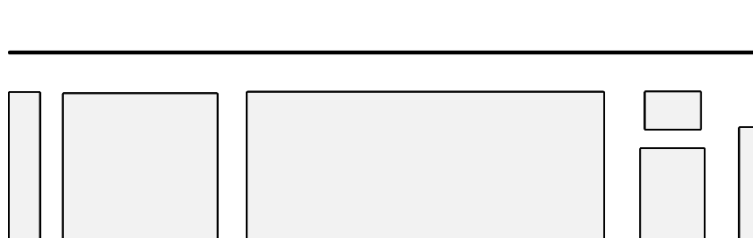


Figure 5: Rough map over scenario A: open corridor.





Figure 6: Scenario A: open corridor with two mid band UEs placed out.

### 3.1.1 Mid band measurements

For the mid band measurements, results from two experiments will be presented. The first experiment is depicted in Figure 7. In this experiment the BS is standing in front of a wall to the right in the map; the UE is starting just in front of the BS. The channel is then collected for 60 seconds as the UE moves away from the BS, along the corridor. The experiment is mostly a Line-of-Sight (LOS) scenario, however due to people moving around in the corridor, some temporary blockage could occur. From this data, the time evolution of different parameters when increasing the distance, such as path loss, in a typical industrial environment can be investigated.

The next experiment analysed is shown in Figure 8. Here, the UE is first moving away from the BS with a LOS link as in the previous measurement. Then the UE is moving around a corner, continuing along another corridor with equipment on both sides. This allows for analysis of the blockage profile when going from LOS to Non Line-of-Sight (NLOS) and time evolution in a NLOS scenario, to be compared to the LOS case.

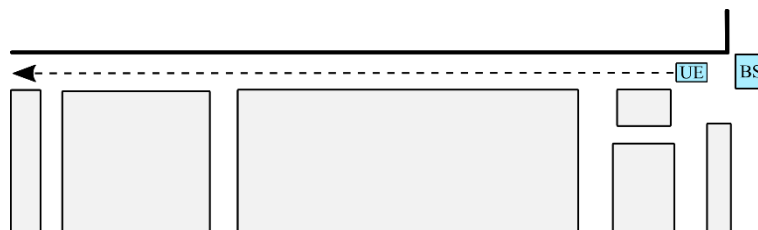


Figure 7: Map over the experiment where the UE is moving in a straight line away from the BS.

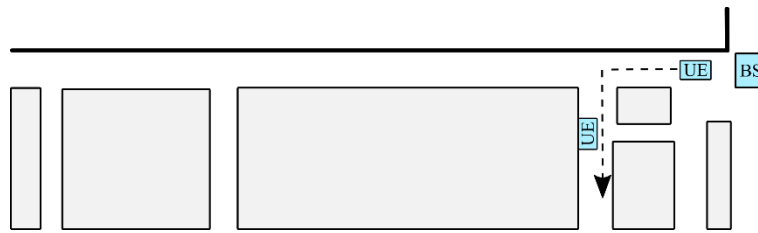


Figure 8: Map over the experiment where the UE is moving in a straight line away from the BS and then in a straight line to the left into a NLOS scenario, passing one static UE.

### 3.1.2 Millimeter-wave measurements

For the mmWave measurements, as similar to the mid band measurements, the channel was collected as the UE was moving away from the BS as seen in Figure 9. The measurement was taken for 18 seconds over a distance where the signal-to-noise ratio was roughly estimated to still be sufficient.

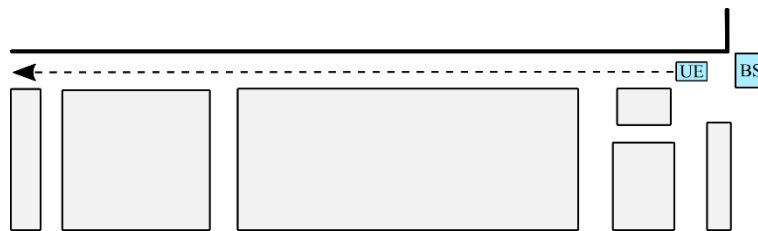


Figure 9: Map over the experiment where the UE is moving in a straight line away from the BS.

## 3.2 Scenario B: semi-open environment with robot interaction

Scenario B includes a semi-open environment in the middle of the area but where high equipment creates corridor-like environments on both sides. This environment is a highly dynamic one as it involves robot interactions of different kinds as well as people walking around and crossing when moving in the room and transporting equipment and products.

This scenario, as roughly shown in Figure 10, was chosen as it is a highly dynamic environment and hence a relevant scenario when analysing challenges in industrial environments from a propagation point of view. The size of the area shown is about 24 x 18 meters. The environment also includes high metallic equipment as well as other materials that could cause different propagation effects; an example of this can be seen in Figure 11. It is a diverse environment, enabling several interesting investigations including, but not limited to: LOS and NLOS measurements, shadowing and blockage profiles from different types of robots as well as humans and transitions from LOS to NLOS.



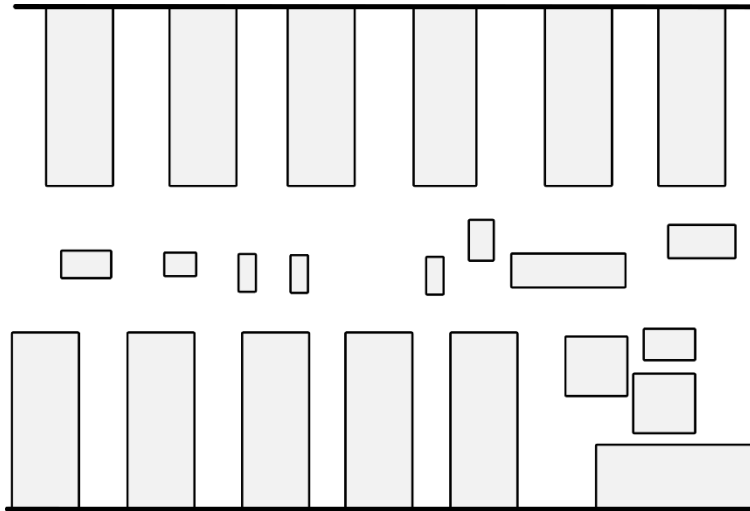


Figure 10: Rough map over scenario B: semi-open environment with robot interaction



Figure 11: View of the semi-open part of the environment.

### 3.2.1 Mid band measurements

In the first experiment of this scenario, the interaction with robots and the resulting blockage profiles were in focus. As seen in Figure 12, the BS is standing towards a wall and the UE is static in the middle of the area. The marked area around the UE is where the robot interactions mostly took place as the robots passed by when performing different tasks in the environment.

In Figure 13 the second experiment is depicted, with the BS in the same place as for the first experiment and the UE moving, first away from the BS with a LOS link and then moving around a corner into NLOS. With this data, the blockage profile when going from LOS to NLOS in a different environment can be investigated. As the factory was fully operating at all times, there is no guarantee that the results also are not influenced by robots and humans moving around.

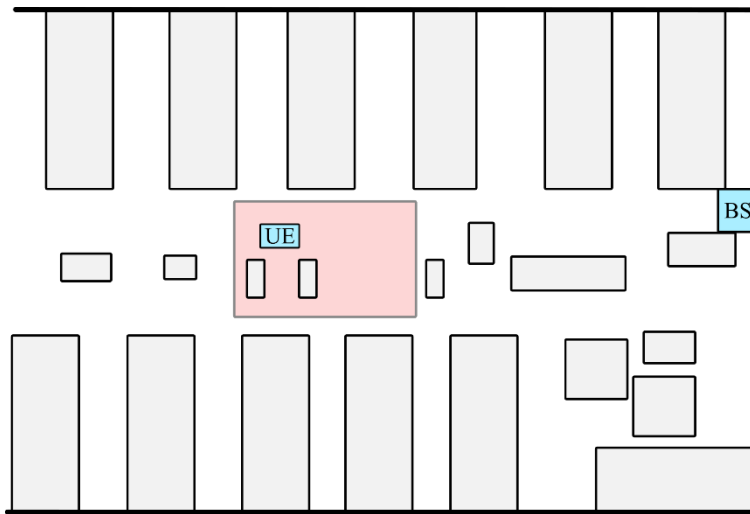


Figure 12: Map over the experiment with a static UE and robot moving in the marked area.

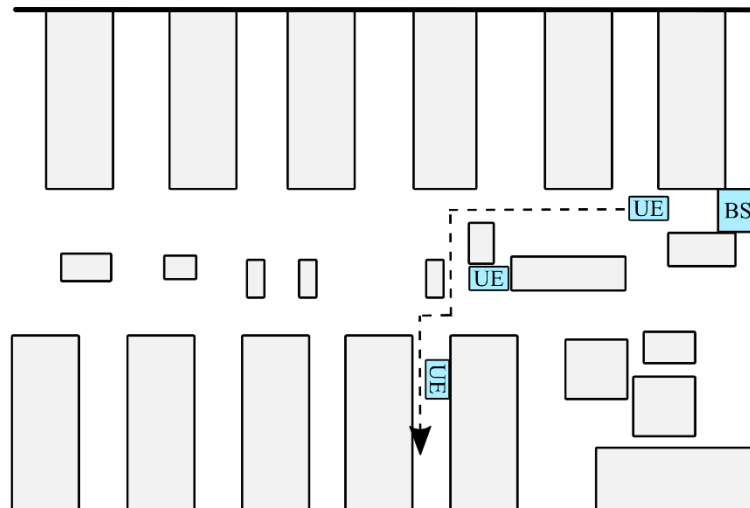


Figure 13: Map over the experiment with two static UEs and one UE moving from LOS to NLOS.

### 3.2.2 Millimeter-wave measurements

The first experiment performed with the mmWave equipment in this environment was a reference measurement seen in Figure 14, performed in a series of static points, where the UE is placed at discrete points along the straight line with a LOS link to the BS.

In Figure 15, the measurement where the UE moves from LOS to NLOS is shown. First the UE is placed in the semi-open environment and is then moved into a quite narrow corridor created by high metallic equipment.

Similar to the mid band measurements, robot interactions were also captured to be able to analyse how this influences the channel on higher frequencies. This analysis was based on different UE positions along the route in Figure 14.

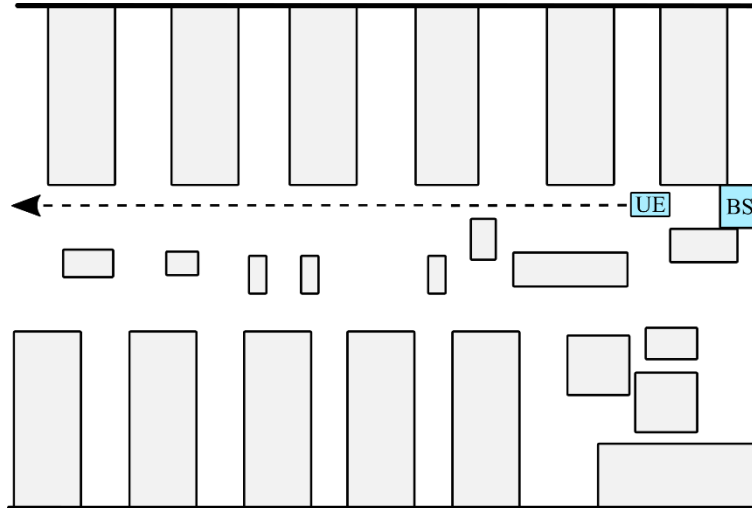


Figure 14: Map over the experiment where the UE is moving in a straight line away from the BS.

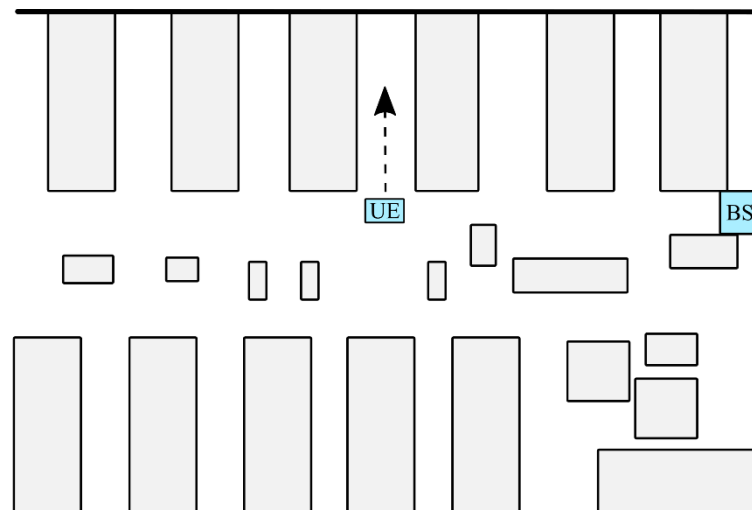


Figure 15: Map over the experiment where the UE is going from LOS to NLOS.

### 3.3 Scenario C: heavy blockage

Scenario C is a scenario, which visually can be characterised by very heavy blockage. The environment is a room containing the backsides of the machinery and hence, there are no robots or humans present unless the machines are in need of maintenance or similar. However, this scenario would be a typical environment for placing sensors to monitor the status of machines and hence, connectivity is still required.

The map in Figure 16 displays the outline of the chosen scenario. The length of the room is approximately 18 meters and the width is about 4 meters. The blocks are tall metallic machinery and

being an environment, which is not used for production, the corridors are very narrow and therefore the room includes many blocked areas and is a very tricky environment for obtaining good coverage everywhere. Figure 17 shows the view towards the mid band BS and gives an idea of the complexity of the environment. Rich scattering due to all the metallic equipment is expected in the environment and there are many possibilities of investigating blockage profiles and coverage in extremely tricky areas.

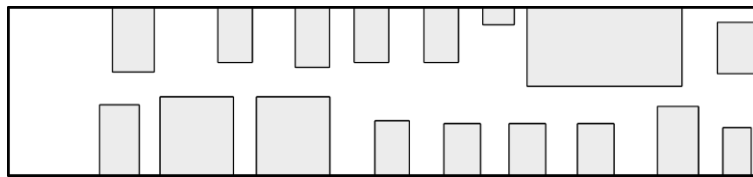


Figure 16: Rough map over scenario C: heavy blockage

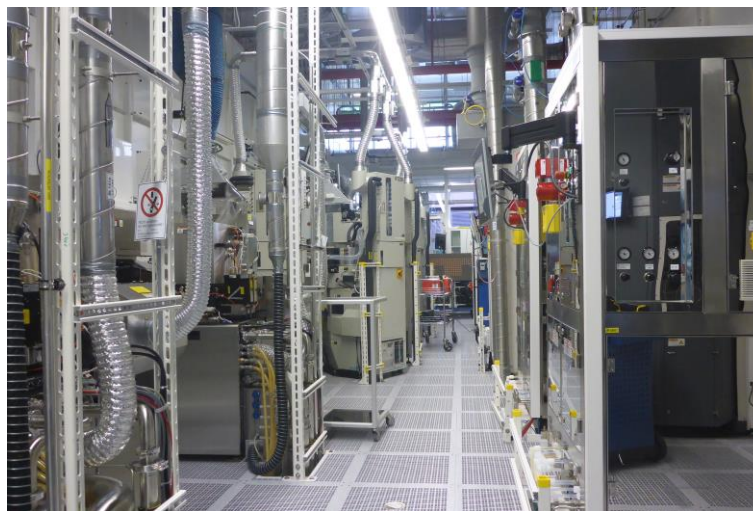


Figure 17: View over the narrow corridor with the mid band measurement equipment in the background.

### 3.3.1 Mid band measurements

To characterise the blockage profile in this environment, continuous measurements were made with the UE moving along the corridor, going into each of the places in between the machinery as in Figure 18. The BS was placed next to the wall in one end of the corridor, with the antennas pointing towards the machinery and the narrow corridor. The route was completed in two runs of 60 seconds each, one starting from the BS side of the corridor and one starting from the other end.

The second type of measurements performed in this scenario is displayed in Figure 19 where the UE starts in the middle of the narrow corridor with a direct link to the BS and then moves into either the left or the right side of the corridor and there is scanning the whole area by moving the UE antennas around. This means that the channel was captured both close to the floor as well as high up; the UE antennas were moved close to the machinery on both sides and even went into tricky places within the blocks in the map, where possible.

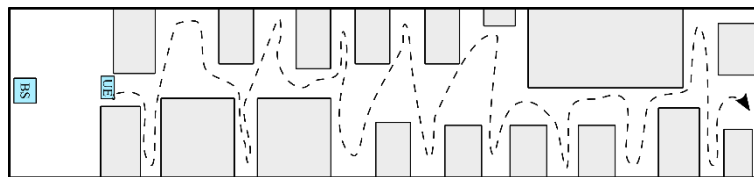


Figure 18: Map over the experiment where the UE is moving along the corridor and while going in and out of shadowed zones.

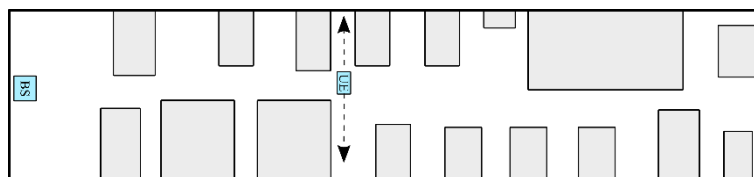


Figure 19: Map over the two experiments where the UE is going from LOS and then into either right or left and scanning the whole area.

### 3.3.2 Millimeter-wave measurements

Static reference measurements were taken by moving the UE a fixed distance along the narrow corridor as in Figure 20. As for the mid band measurements, the BS was placed at the end of one side of the corridor. Being a rich scattering environment, it is relevant to investigate the behaviour of MPCs to find out exactly how rich scattering it is and what the angular spread is.

Investigating the LOS to NLOS transition, the transmitter was moved from one NLOS position on one side of the corridor, passing through the middle where there is LOS and then into a NLOS region again, see Figure 21. This results in two transitions and hence, two blockage profiles caused by heavy machinery.

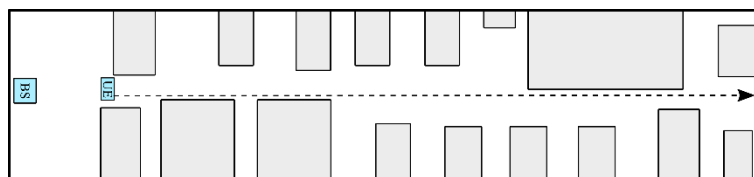


Figure 20: Map over the experiments where the UE is moving in a straight line away from the BS.

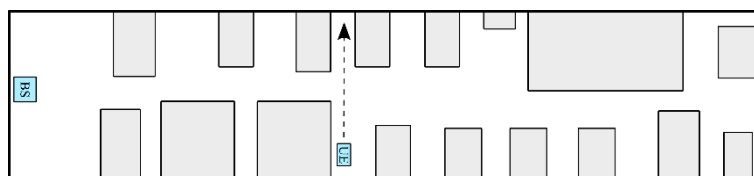


Figure 21: Map where the UE is moving from NLOS to LOS and then to NLOS again.

## 4 Channel characteristics

In this section the results from the channel measurements are presented, starting with the mid band measurements and continuing with the mmWave measurements. Pictures from the actual

measurements are included, followed by the corresponding results, analysis and implications for an implementation in a real operating factory.

#### 4.1 Mid band characteristics

For the mid band measurements, channel characteristics such as the received power over distance, blockage profiles, fading characteristics and polarisation aspects are investigated. Results will be presented both when using the planar array but also when using the distributed setup as described in section 2.1.

##### 4.1.1 Scenario A: open corridor

The first scenario presented is scenario A, which includes an open corridor and is shown in Figure 6. The first experiment is seen in Figure 7 and includes one UE moving along the corridor, away from the BS. The BS is located in one end of the corridor and next to the wall, see Figure 22. The vicinity of the BS is fairly open, in comparison to most locations in the factory, but there are metallic racks with boxes nearby and people could pass by when performing their tasks. The view towards the UE is seen in Figure 23, which also gives an idea about the reflective environment that includes a lot of metall but also other types of materials.



Figure 22: View towards the BS.





Figure 23: View towards the UE.

The received channel gain, averaged over frequency, at the BS side as the UE moves away is depicted in Figure 24. Over the distance that the channel measurements were collected, the received channel gain decreased from about 17 dB to almost -15 dB. One of the UE antennas is physically oriented to have a vertical polarisation while the other is oriented to have a horizontal polarisation. The channel gain as received by the two different polarisations are similar, although one is occasionally stronger than the other depending on where the UE is and what MPCs that are contributing at the moment.

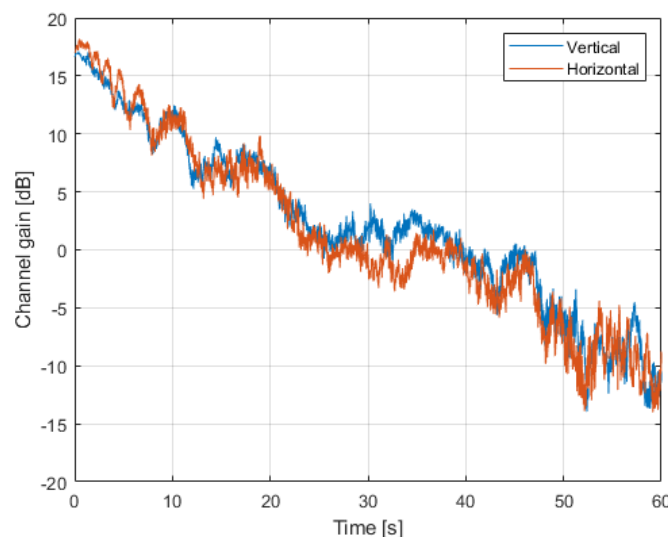


Figure 24: Received channel gain over time when using a vertical and a horizontal UE antenna, respectively.

The second experiment for this scenario is shown in Figure 8 and includes a transition from LOS to NLOS. The BS is placed at the same place as before and the view of the UE in LOS also remains the same. The view when going around the corner can be seen in Figure 25.





Figure 25: View towards the UE after turning around the corner, with the BS being to the left.

The received channel gain over time is shown in Figure 26 for both UE polarisations. As expected, the path loss for the first 5-7 seconds are similar to the one in the previous experiment, as it is the same path. Then when moving around the corner the received channel gain drops with about 5 dB, the horizontal before the vertical one. This is most likely an effect caused by self-blockage from the rest of the UE and influence by the antenna pattern as the LOS link is lost earlier on and then the horizontal polarisation has to rely on reflections. After that the received channel gain continues to decrease as the UE move further away, however not as fast as in LOS. Interesting to note is that, for some reason, the channel gain slope for the vertical polarisation is decreasing faster than for the horizontal one in NLOS.

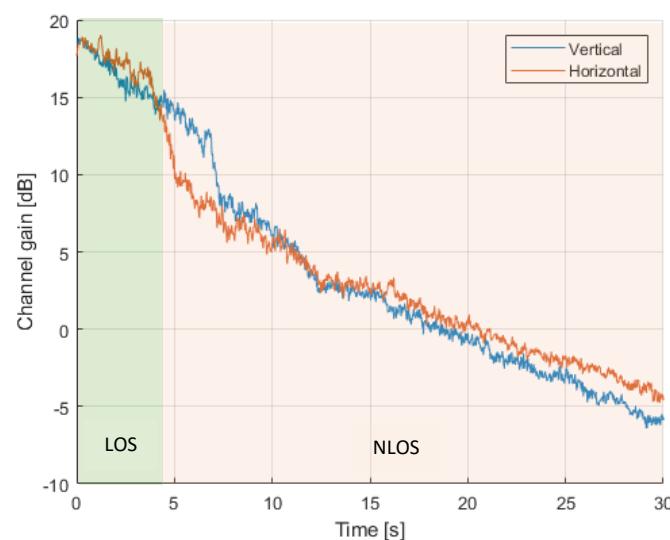


Figure 26: Received channel gain over time when using a vertical and a horizontal UE antenna, respectively, first in LOS and then in NLOS.

#### 4.1.2 Scenario B: semi-open environment with robot interaction

The second scenario presented is scenario B, which is a very dynamic semi-open environment, including a lot of robot interactions as well as interactions from humans. Starting with the

experiment shown in Figure 12 where there is a static UE and robots are moving around the UE, on different routes, and creating shadowing effects. Two different measurements with robot interactions will be presented here.

As seen in the map in Figure 12, the BS is positioned against the wall; the view towards the BS can be seen in Figure 27. To the left in the figure, a robot, which moves back and forth in the environment, can be seen and in the ceiling, there are tracks where material is transported. Note that the UE positioned in front of the BS in the figure was not present for these measurements.



Figure 27: View towards the BS.

The measurements, aiming at capturing the dynamics caused by robot interaction, were 30 seconds long. The view toward the UE after 8, 17 and 22 second are seen in Figure 28, Figure 29 and Figure 30, respectively. In Figure 28, there is a robot approaching the UE from the other side of the room. Figure 29 shows the situation after around 17 seconds, including two robots where one is about to cross right in front of the UE and hence blocking the LOS link. After around 22 seconds the robots are still circulating around the UE and this situation is depicted in Figure 30.



Figure 28: View towards the UE after around 8 seconds.



Figure 29: View towards the UE after around 17 seconds.



Figure 30: View towards the UE after around 22 seconds.

The resulting received channel gain over time from these robot interactions can be seen in Figure 31, for both UE polarisations. In the beginning, the channel variations, as averaged over frequency, are minor. When the first robot is approaching the variations increase, most likely due to that the scattering in the near vicinity of the UE is changing, where the metallic robots are acting as reflectors. When one robot passes in between the BS and the UE, the received channel gain drops with 4-6 dB depending on the polarisation of the UE antenna. In the last part of the measurement, when multiple robots were circulating around the UE, the channel gain varies even more than before as the highly reflective close-by scattering points are changing fast. With these changes, the channel gain can go up and down with 3-5 dB within a short time interval.

This measurement captured a quite complicated scenario with both heavy blocking and highly reflective scatterers in the near vicinity of the UE. However, even with the heavy blocking, only a drop of 4-6 dB is experienced after applying maximum ratio combining on the signals received and adding up all the antennas in the massive MIMO array. The margin that needs to be accounted for due to close-by moving scatterers is in this measurement 3-5 dB and overall the results are quite promising for massive MIMO to be able to handle complex situations in a highly dynamic industrial scenario.

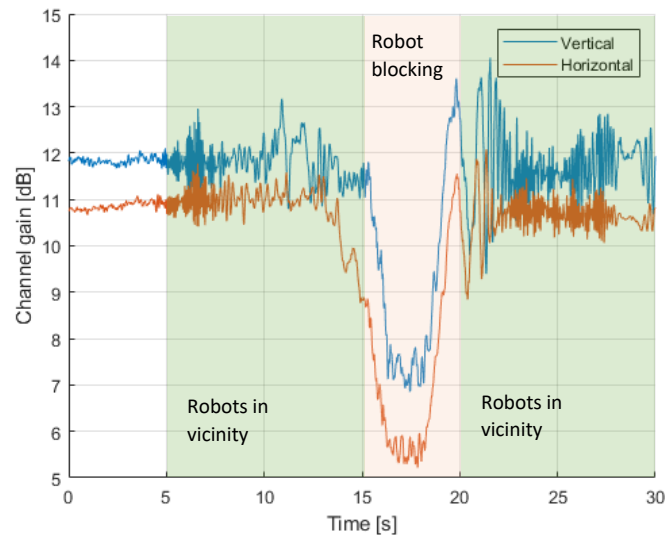


Figure 31: Received channel gain over time when using a vertical and a horizontal UE antenna, respectively.

The next measurement, which also is from an experiment including robot interactions, but also interactions from humans, lasted for 30 seconds as well. After around 5 seconds, a robot passed by between the BS and UE and hence blocked the LOS. In the second half of the measurement, around 18 seconds, a human crossed in front of the UE, continuing on the path from the UE towards the BS and therefore continuing to influence the channel.



Figure 32: View towards the UE after around 5 seconds.



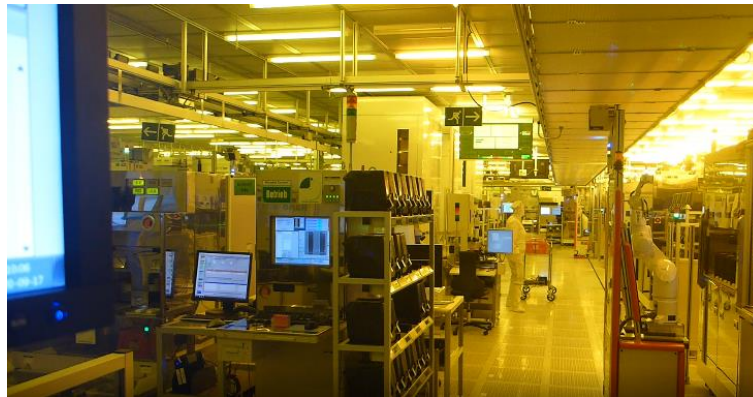


Figure 33: View towards the UE after around 18 seconds.

The received channel gain at the BS side for this measurement is seen in Figure 34 for both UE polarisations. Interesting to note is that the average channel gain is higher for the horizontal polarisation than the vertical one, which potentially could be due to reflections from the ground or ceiling. The drop caused by blockage of a robot is 3-5 dB depending on the initial level of channel gain for the two UE polarisations. The corresponding drop when the human initially blocked the LOS is approximately 2 dB and is followed by some variations up and down as the human moves along the path from the UE towards the BS. However, the changes are quite smooth in comparison to having a highly reflective scatterer circulating around nearby, as seen in Figure 31.

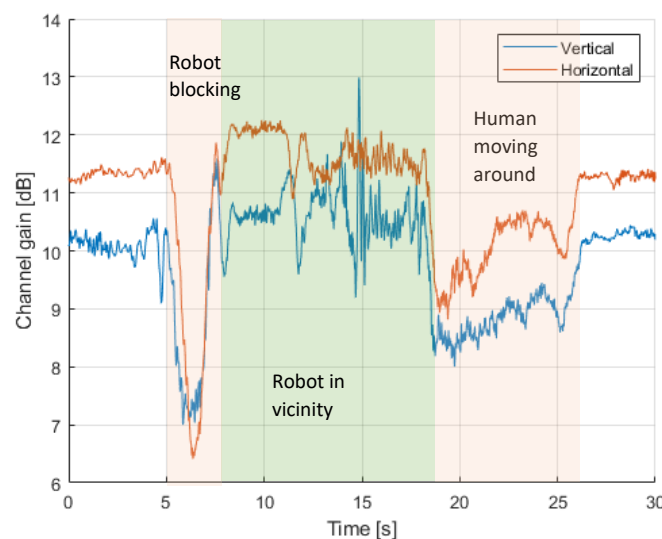


Figure 34: Received channel gain over time when using a vertical and a horizontal UE antenna, respectively

The last experiment in this scenario is seen in Figure 13 and includes a transition from LOS to NLOS when moving around a corner and continuing further down that path. The view after just turning around the corner can be seen in Figure 35 and later on when entering a different part of the room, the view is as in Figure 36. The path is quite diverse in terms of different width of corridors, which also is changing due to equipment and materials along the way. Variations are also caused by humans working.



Figure 35: View towards the UE after turning around the corner.



Figure 36: View towards the UE after turning around the corner, further down the path.

The total path loss from start to end of the measurement is around 14 dB for the two UE polarisations. The blockage profile due to the transition from LOS to NLOS is quite smooth in comparison to blockage due to robot interactions, as previously seen in Figure 31 and Figure 34. Also as previously observed, the channel gain in NLOS decrease slower than in LOS when moving away from the BS.

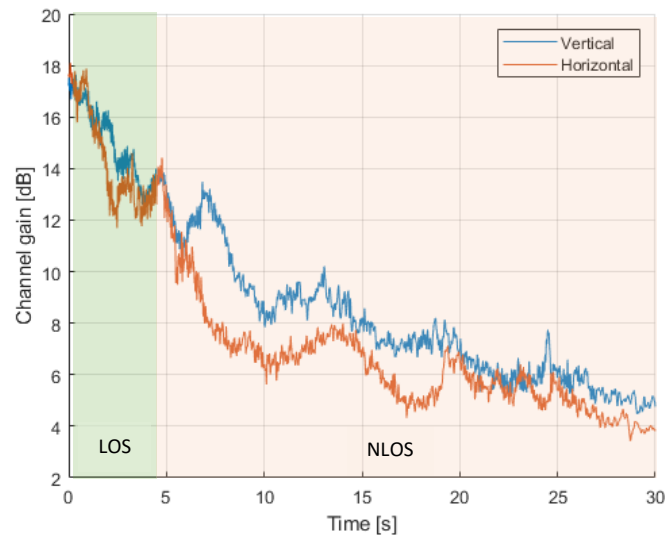


Figure 37: Received channel gain over time when using a vertical and a horizontal UE antenna, respectively.

#### 4.1.3 Scenario C: heavy blockage

The last scenario is scenario C that is a highly reflective environment with lots of high metallic equipment and narrow corridors. In general the environment is not a dynamic one, since there is no production in the area and for these measurements only the person moving the UE could have influenced the channel. In Figure 38, the view toward the BS when having the centralised array deployed. The width of the central corridor in this scenario is about the same width as the array. The case when the distributed array is deployed is seen in Figure 39. Two white boards were used to enable the deployment of a fully, within cable limitations, distributed setup with random orientations of the antennas.



Figure 38: View towards the BS, deployed with the centralised array.



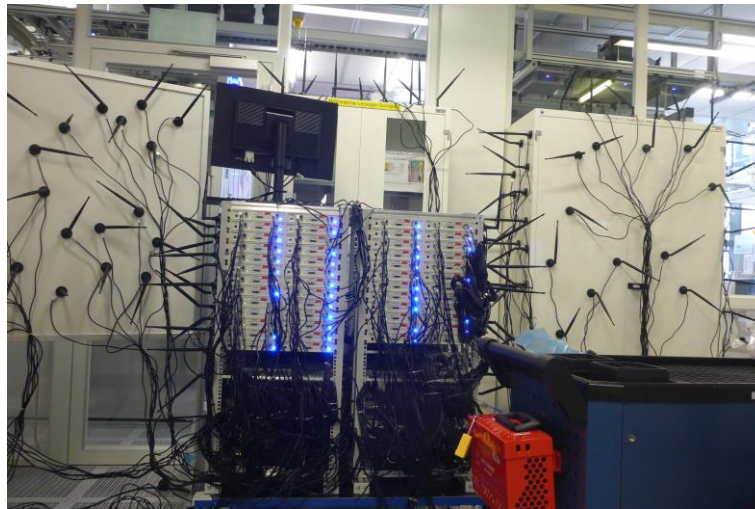


Figure 39: View towards the BS, deployed with the distributed array.

The first experiment for this scenario is seen in Figure 18 and for this experiment the UE was moving along the corridor while going in and out of the shadowed areas to both the left and right. The resulting channel will therefore include both path loss and blockage profiles. The view towards the UE when it is in the narrow corridor is seen in Figure 40.



Figure 40: View towards the UE.

When having the centralised array deployed, the received channel gain looks like in Figure 41 for the two UE polarisations and the five shadowed areas closest to the BS. What is in the figure are five



very clear peaks and dips when alternating between LOS and NLOS. Depending on how far away from the BS the UE is, the drop is at its extreme approximately 10 dB and then later on 5-8 dB for these distances. What can also be observed is that even though the two UE polarisations behave similarly, there are still some differences where the peaks are shifted in relation to the other polarisation. In general, the vertical polarisation is stronger for a longer time. Causes for these differences could be due to self-blockage of the horizontal polarisation when moving the UE and influence by the antenna pattern.

In Figure 42, the results of the corresponding measurements when deploying the distributed setup is shown for both UE polarisations. Note that overall, the received channel gain is lower, which is due to using BS antennas with lower gain and an extra five meter cable to connect them. Here, the largest dip is about 8 dB and the others 3-5 dB depending on the distance. In general, the variations of channel gain over time is smaller with the distributed setup in comparison to the centralised setup.

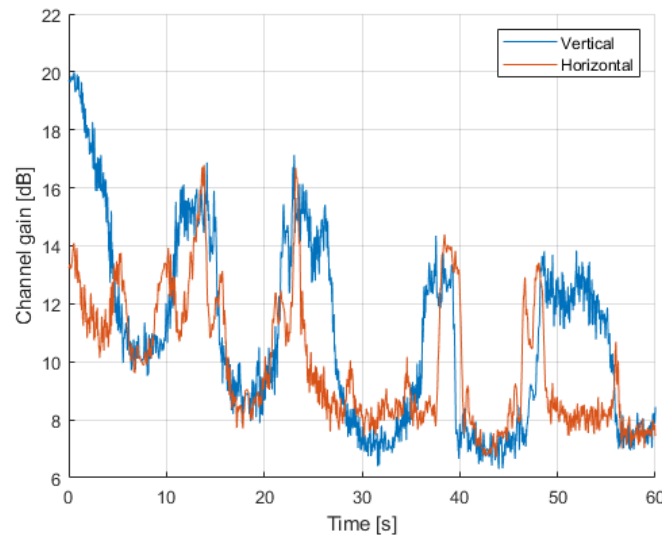


Figure 41: Received channel gain over time when using a vertical and a horizontal UE antenna, respectively.

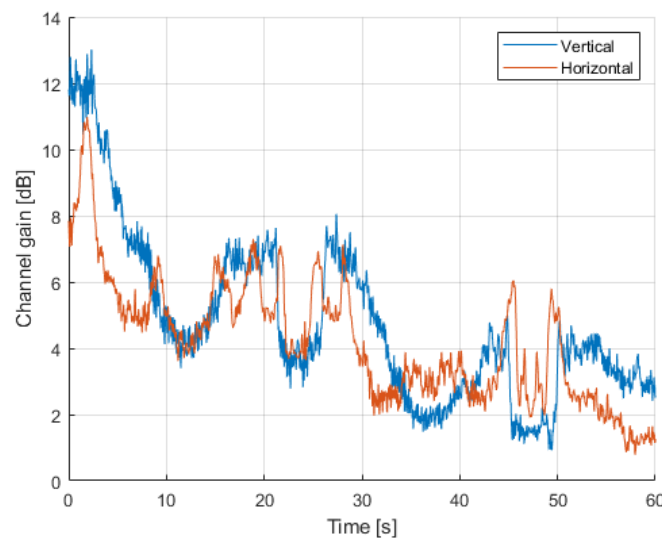


Figure 42: Received channel gain over time when using a vertical and a horizontal UE antenna, respectively.

The second experiment, as shown in Figure 19, starts with the UE centered in the narrow corridor with LOS conditions. Then the UE was moved into a shadowed area, either to the slightly wider area on the right or the more narrow area on the left, as seen from the BS. In Figure 43, the view when scanning the shadowed area to the right is seen. The experiment was done for both the centralised and the distributed setup.



Figure 43: View towards the UE when scanning the shadowed area on the right side of the corridor.

Starting with the centralised array and investigating the channel gain, normalised such that the average antenna has a power of 1, over time and frequency, the results look as in Figure 44 for the vertical UE antenna. The lower part of the figure shows the channel gain when using the vertical antenna in the upper left corner of the array as an example. For this antenna the channel gain is varying more than 20 dB over both time and frequency. The upper part of the figure shows the channel gain when applying maximum ratio combining to the signals and adding up the contributions from the 100 antennas. For this case, a slightly higher channel gain can be seen in the beginning, as the UE antenna is in LOS, and after that it goes down and reaches a quite flat level, which is stable over both time and frequency. This effect is called channel hardening and is a result of combining the many antennas in a massive MIMO system. With the channel hardening effect, the reliability of a system can be increased and the fading margins reduced due to the more stable channel gain. Adding up all the antennas also result in a higher total channel gain – the array gain – that can be exploited by either extending the coverage or lowering the UE transmit power with a factor corresponding to the number of antennas.

Exploring the same data but from another angle, the empirical CDF of the channel gain is shown in Figure 45 for 1 and 100 antennas respectively. Naturally, the steeper the curve is, the more channel hardening. For the 100 antenna case, which is normalised by the number of antennas for comparison, the curve is quite steep and the tail of the curve is small. On the other hand, for the 1 antenna case the curve is not as steep and the tail is quite significant, making the channel gain more unpredictable and the system needs to cover a wider range and have a much higher sensitivity in order to reduce the probability of outage.

The third point of view in which this data will be displayed is when zooming in to the question regarding what fading margin would be required to have in a system operating in this type of environment. In Figure 46 the data from Figure 44 is seen again for the 100 antenna case, as averaged over frequency. Here it can be more evidently seen that the blockage occurring from the LOS to NLOS transition is approximately 6 dB. Then the variation around this new mean is not much more than only 2 dB from top to bottom and the channel remains quite stable throughout the whole scanned area.

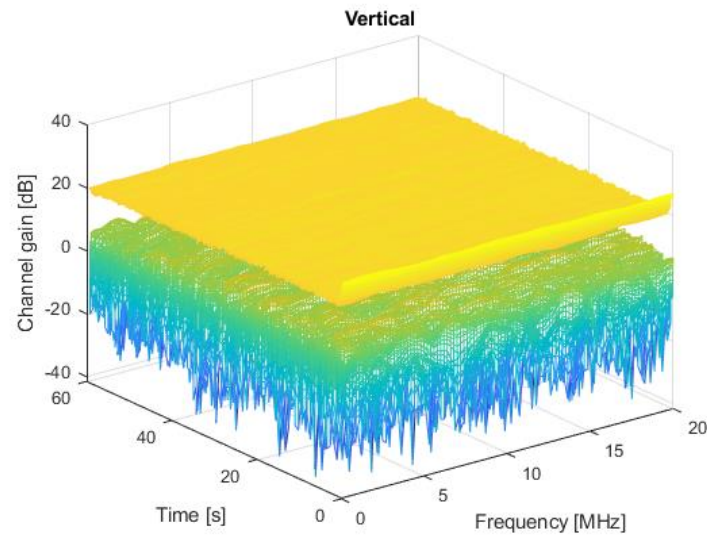


Figure 44: Channel gain over time and frequency for the vertically polarised UE antenna when scanning the shadowed area on the right side of the corridor using 1 (lower) and 100 (upper) antennas of the centralised array, respectively.

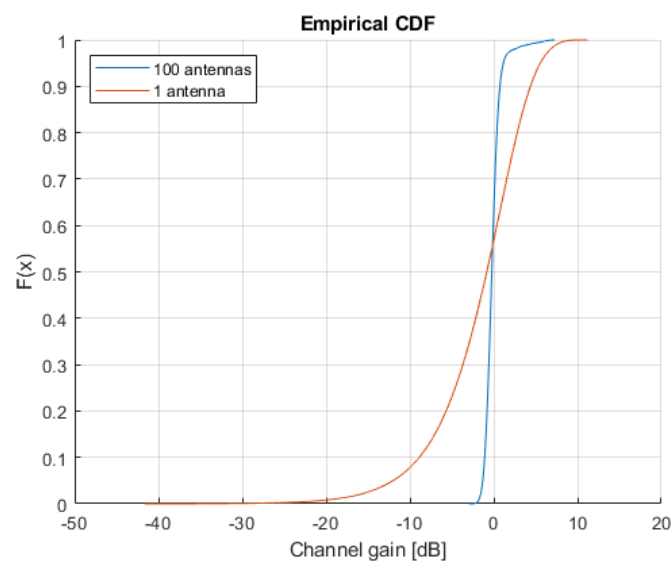


Figure 45: Empirical CDF for 1 and 100 antennas of the centralised array, respectively, when scanning the shadowed area on the right side of the corridor with a vertical UE antenna.

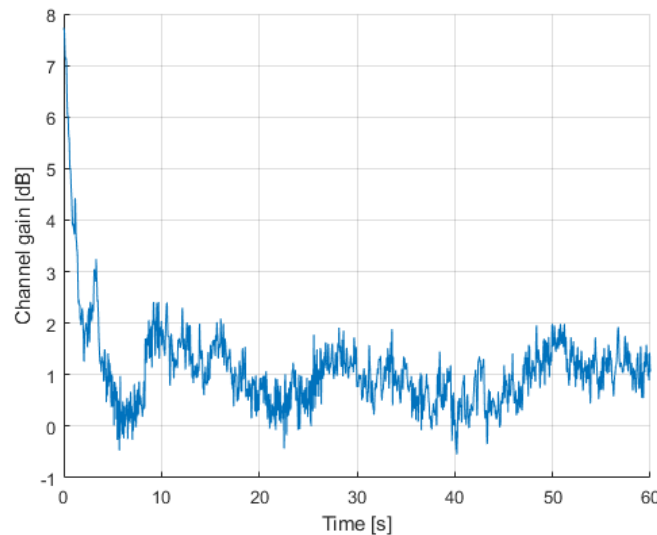


Figure 46: Channel gain over time, averaged over frequency, for 100 antennas in the centralised array when scanning the shadowed area on the right side of the corridor with a vertical UE antenna.

In Figure 47, Figure 48 and Figure 49, the corresponding results are shown but for the horizontally polarised UE antenna. Observations to be made are that in Figure 47, there are slightly more variations in the time domain. However, it is still quite flat. The horizontal antenna also seems to have been in LOS a bit longer than the vertical one, which is reflected in the curve in Figure 48 where the result for the 100 antenna case results in a peculiar bend at the end. Lastly, in Figure 49, the slightly larger variations originating from the time domain can be seen and a fading margin of 3 dB.

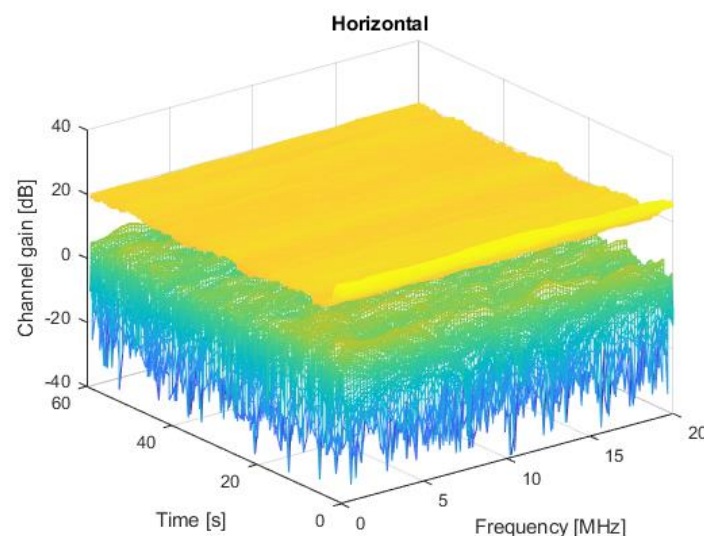


Figure 47: Channel gain over time and frequency for the horizontally polarised UE antenna when scanning the shadowed area on the right side of the corridor using 1 (lower) and 100 (upper) antennas of the centralised array, respectively.



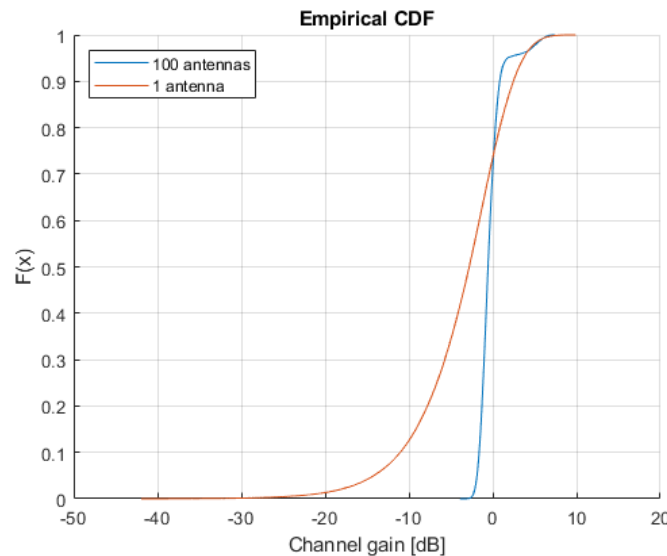


Figure 48: Empirical CDF for 1 and 100 antennas of the centralised array, respectively, when scanning the shadowed area on the right side of the corridor with a horizontal UE antenna.

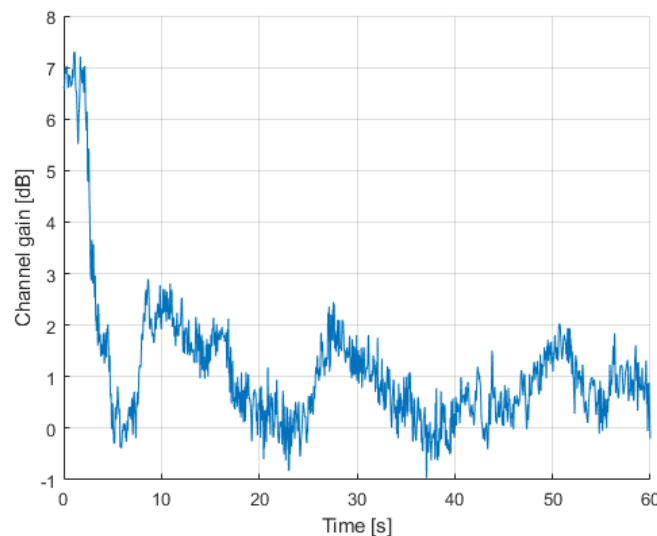


Figure 49: Channel gain over time, averaged over frequency, for 100 antennas in the centralised array when scanning the shadowed area on the right side of the corridor with a horizontal UE antenna

The corresponding experiment was also done for the distributed setup and the corresponding results are to be seen in Figure 50, Figure 51 and Figure 52 for the vertical UE antenna. The results are similar as for the centralised array but some things are worth noting. First of all, with the centralised array there is a clear LOS to each BS antenna as the link is in the direction of the main gain of each antenna in the beginning of the measurement. For the distributed setup this is not the case as many of the antennas are in NLOS and do not have the main gain of their antenna pattern pointing towards the UE. Hence, the dip in the beginning of the measurement when moving from the corridor into behind the equipment is less prominent and hence another dip is seen in Figure 50,



which actually is due to the UE antenna moving into an especially tricky corner behind the equipment. Also due to the less prominent LOS, and hence almost removed blockage profile, the channel gain fits within a range of only 4 dB for the whole measurement, as seen in Figure 52.

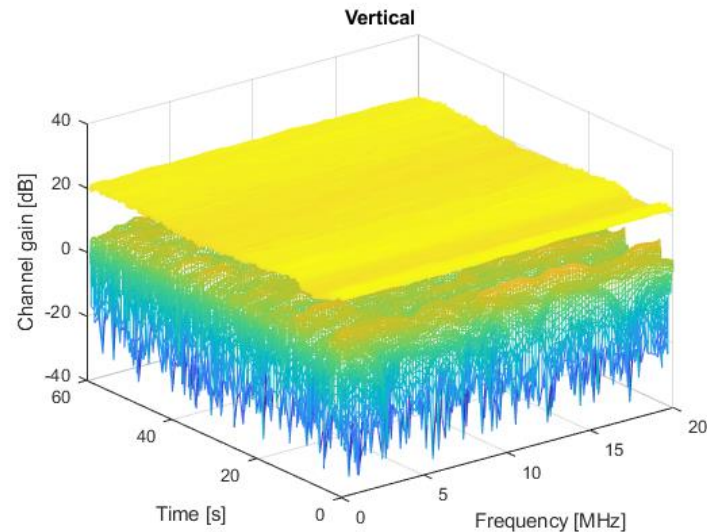


Figure 50: Channel gain over time and frequency for the vertically polarised UE antenna when scanning the shadowed area on the right side of the corridor using 1 (lower) and 100 (upper) antennas of the distributed array, respectively.

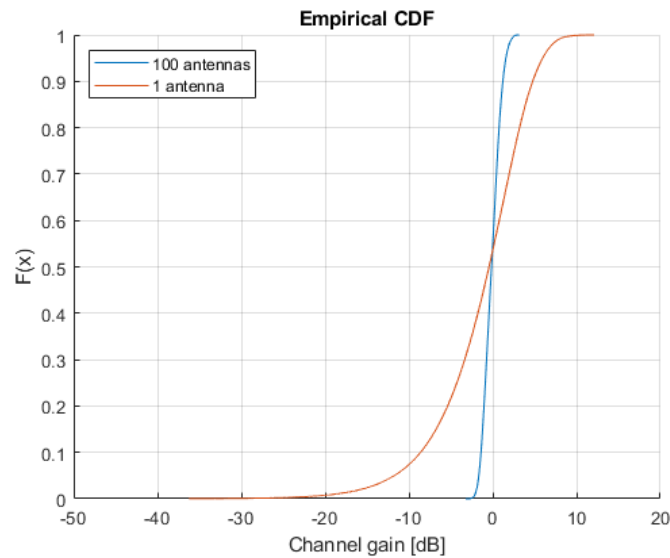


Figure 51: Empirical CDF for 1 and 100 antennas of the distributed array, respectively, when scanning the shadowed area on the right side of the corridor with a vertical UE antenna.

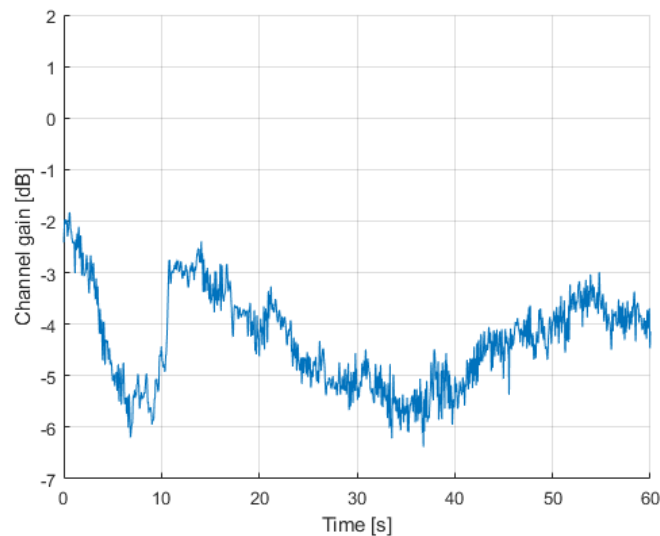


Figure 52: Channel gain over time, averaged over frequency, for 100 antennas in the distributed array when scanning the shadowed area on the right side of the corridor with a vertical UE antenna.

For the distributed setup, the corresponding results for the horizontally polarised UE antenna is seen in Figure 53, Figure 54 and Figure 55. The results are very similar to the case for the vertical UE antenna, although there seems to be more antennas having a close to horizontal polarisation with a LOS link to the UE when placed in the middle of the corridor.

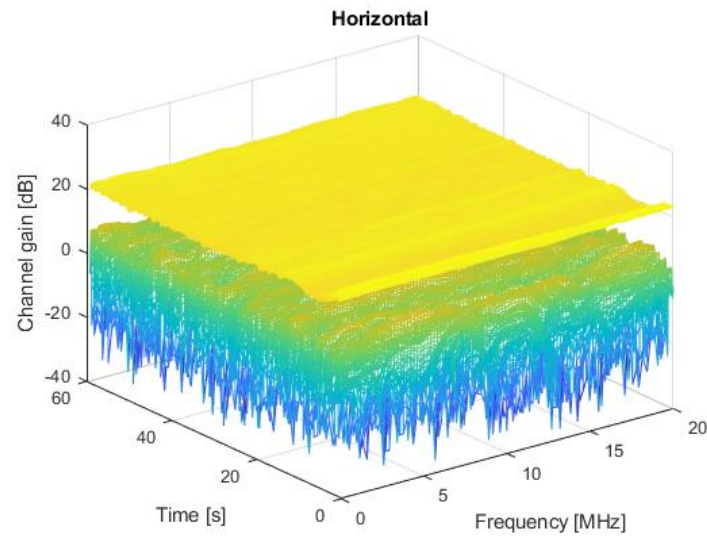


Figure 53: Channel gain over time and frequency for the horizontally polarised UE antenna when scanning the shadowed area on the right side of the corridor using 1 (lower) and 100 (upper) antennas of the distributed array, respectively.

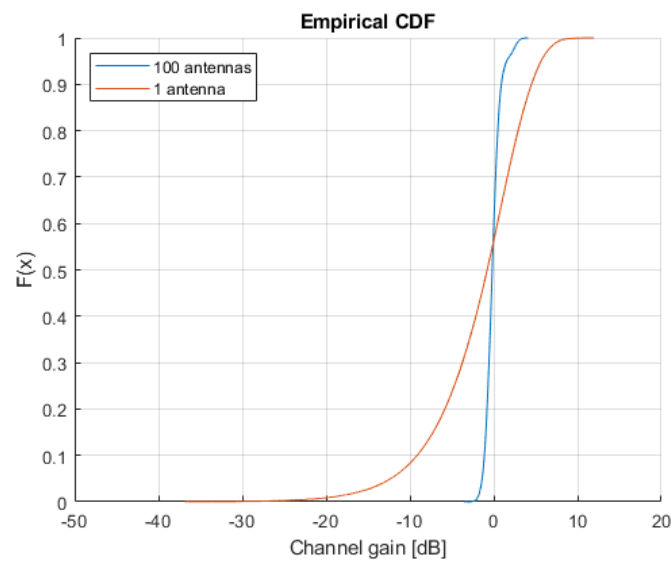


Figure 54: Empirical CDF for 1 and 100 antennas of the distributed array, respectively, when scanning the shadowed area on the right side of the corridor with a horizontal UE antenna.

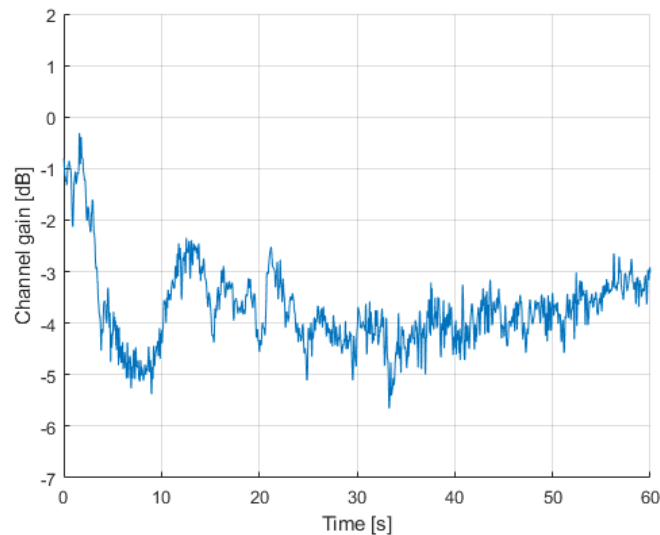


Figure 55: Channel gain over time, averaged over frequency, for 100 antennas in the distributed array when scanning the shadowed area on the right side of the corridor with a horizontal UE antenna

The same scanning experiment was done when also starting in the middle of the corridor but instead moving into the shadowed area to the left and scanning the whole space. In comparison to the previously analysed area, this one is more narrow and the equipment more compact. The experiment was done with both the centralised and the distributed setup.



Figure 56: View towards the UE when scanning the shadowed area on the left side of the corridor.

The figures for the centralised array and vertically polarised UE antenna is depicted in Figure 57, Figure 58 and Figure 59 and for the horizontally polarised UE antenna in Figure 60, Figure 61 and Figure 62. For both cases the results are very similar as when scanning the shadowed area to the right even though this area at first sight seems to be more complicated for the signal to reach at first sight.

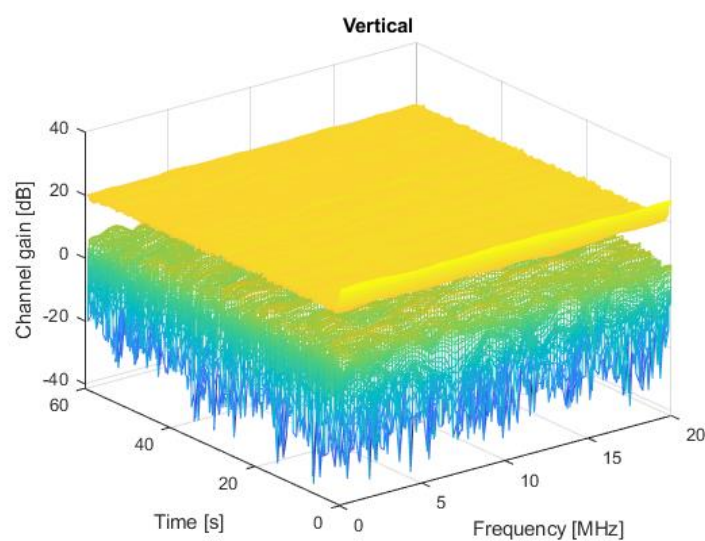


Figure 57: Channel gain over time and frequency for the vertically polarised UE antenna when scanning the shadowed area on the left side of the corridor using 1 (lower) and 100 (upper) antennas of the centralised array, respectively.



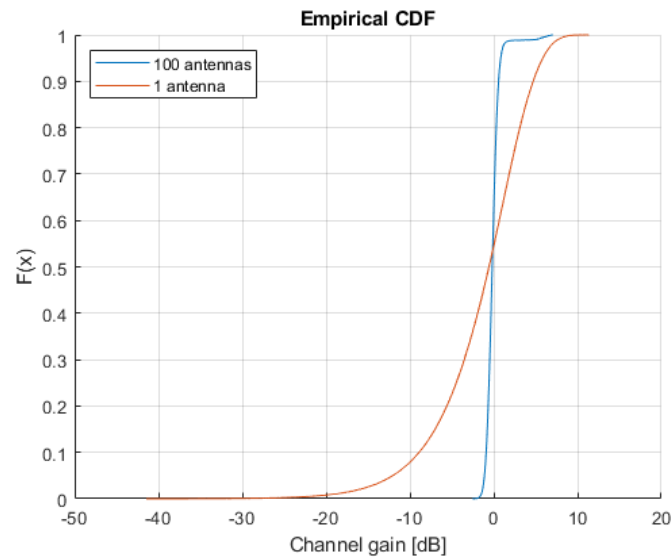


Figure 58: Empirical CDF for 1 and 100 antennas of the centralised array, respectively, when scanning the shadowed area on the left side of the corridor with a vertical UE antenna.

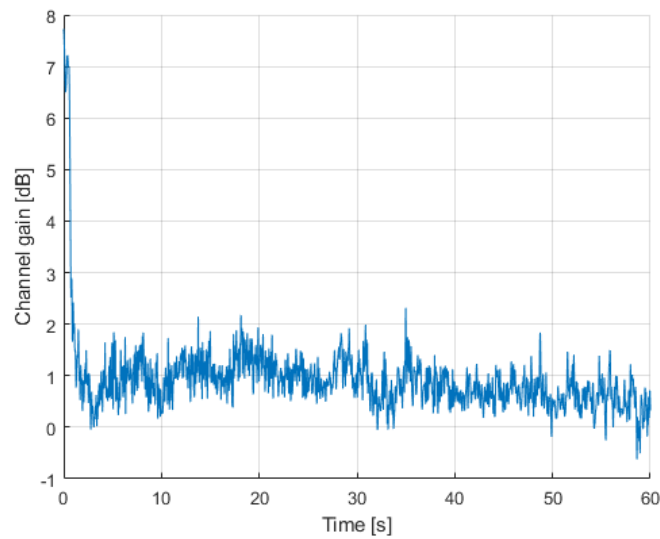


Figure 59: Channel gain over time, averaged over frequency, for 100 antennas in the centralised array when scanning the shadowed area on the left side of the corridor with a vertical UE antenna

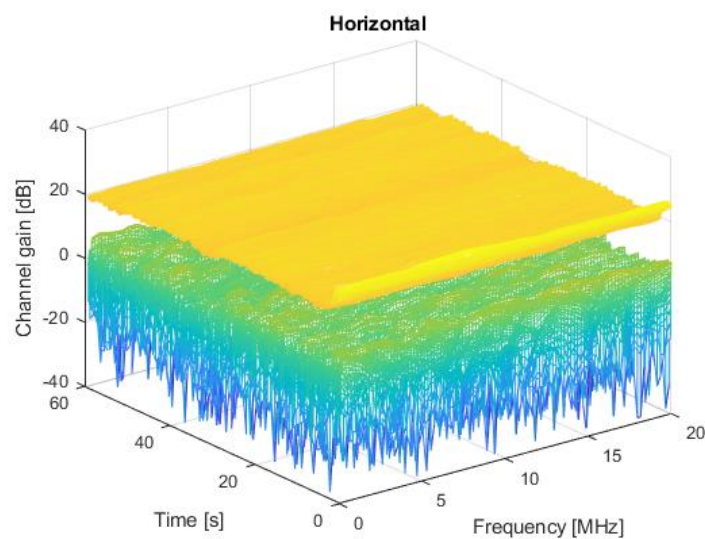


Figure 60: Channel gain over time and frequency for the horizontally polarised UE antenna when scanning the shadowed area on the left side of the corridor using 1 (lower) and 100 (upper) antennas of the centralised array, respectively.

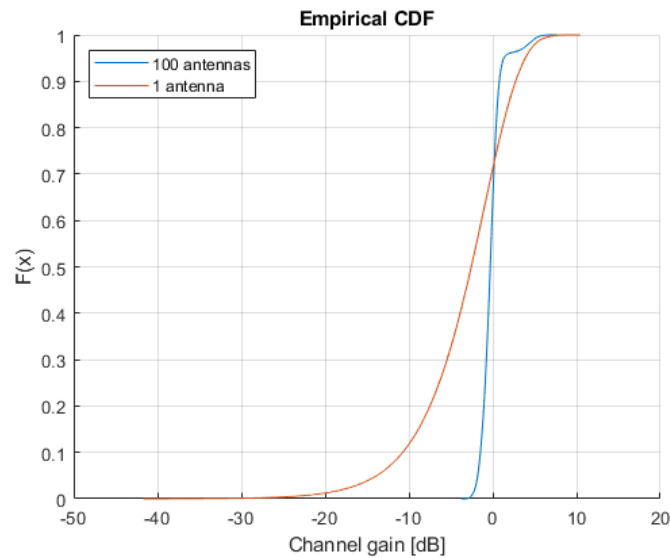


Figure 61: Empirical CDF for 1 and 100 antennas of the centralised array, respectively, when scanning the shadowed area on the left side of the corridor with a horizontal UE antenna.

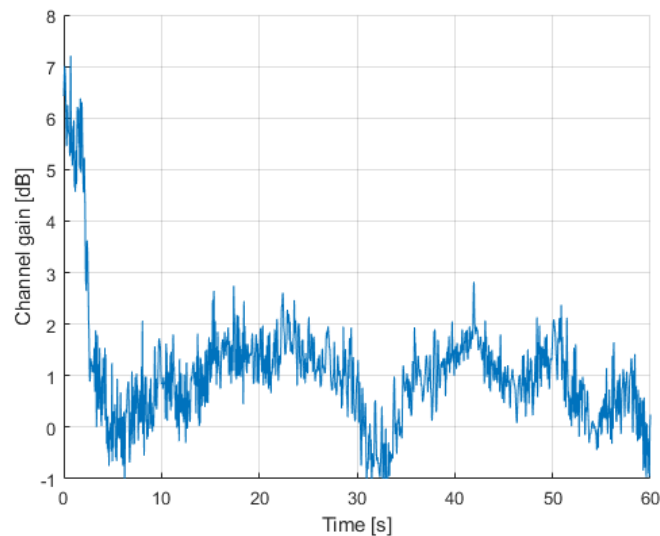


Figure 62: Channel gain over time, averaged over frequency, for 100 antennas in the centralised array when scanning the shadowed area on the left side of the corridor with a horizontal UE antenna

The corresponding results for the distributed setup is seen in Figure 63, Figure 64 and Figure 65 for the vertical UE antenna and in Figure 66, Figure 67 and Figure 68 for the horizontal UE antenna. Also for the distributed setup, the results are similar to those obtained when scanning the shadowed area to the right in the corridor.

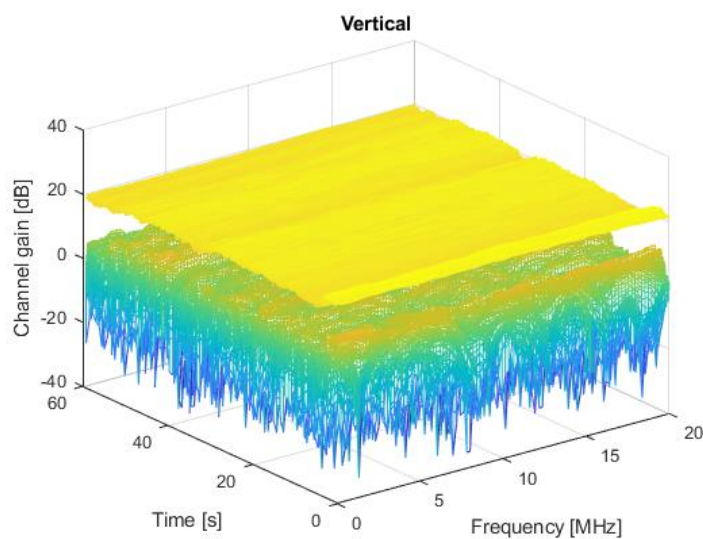


Figure 63: Channel gain over time and frequency for the vertically polarised UE antenna when scanning the shadowed area on the left side of the corridor using 1 (lower) and 100 (upper) antennas of the distributed array, respectively.

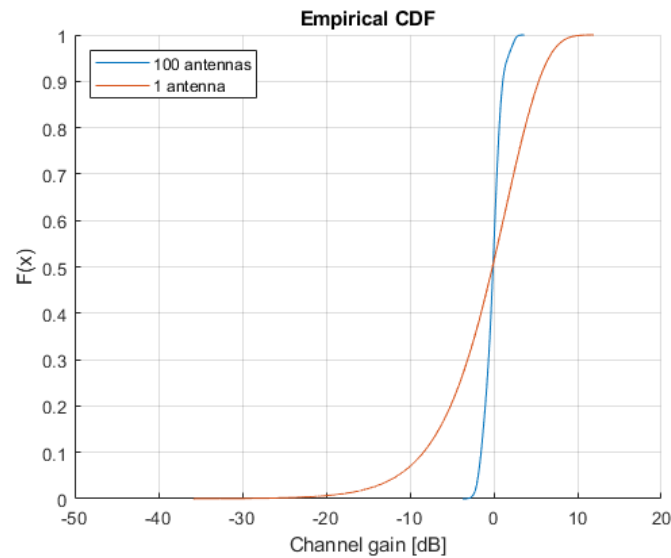


Figure 64: Empirical CDF for 1 and 100 antennas of the distributed array, respectively, when scanning the shadowed area on the left side of the corridor with a vertical UE antenna.

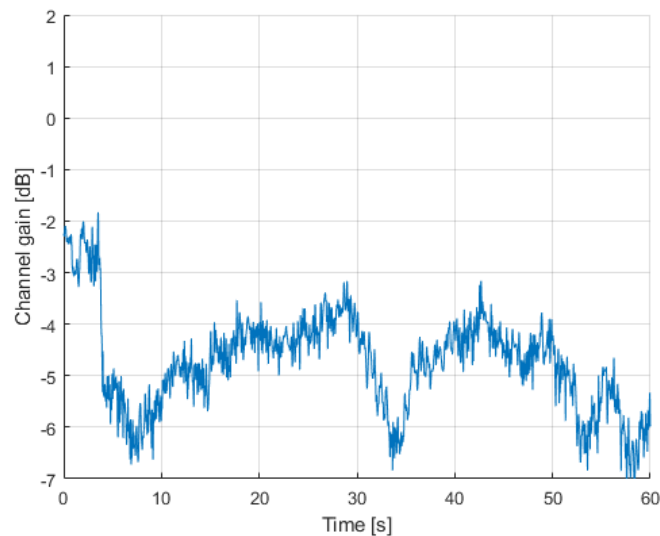


Figure 65: Channel gain over time, averaged over frequency, for 100 antennas in the distributed array when scanning the shadowed area on the left side of the corridor with a vertical UE antenna

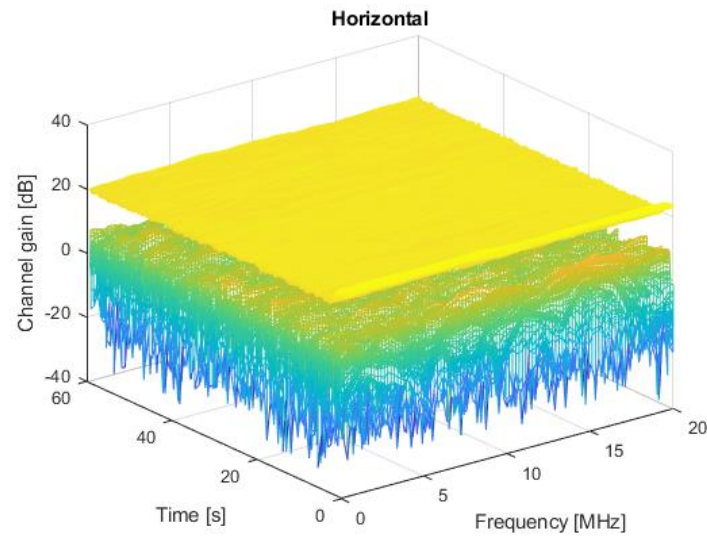


Figure 66: Channel gain over time and frequency for the horizontally polarised UE antenna when scanning the shadowed area on the left side of the corridor using 1 (lower) and 100 (upper) antennas of the distributed array, respectively.



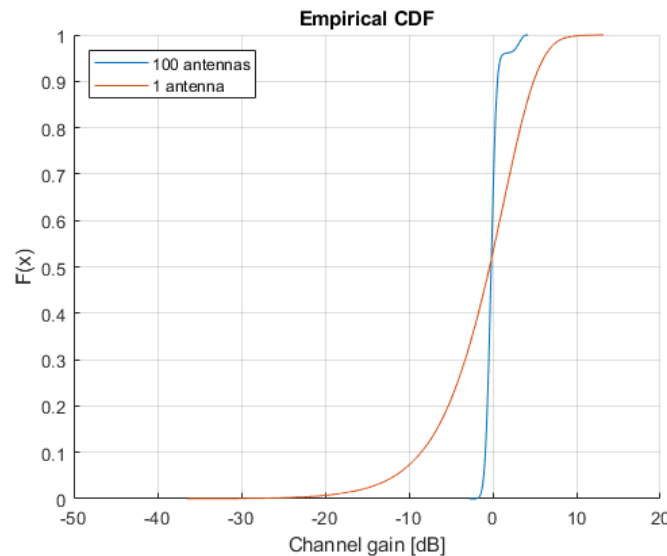


Figure 67: Empirical CDF for 1 and 100 antennas of the distributed array, respectively, when scanning the shadowed area on the left side of the corridor with a horizontal UE antenna.

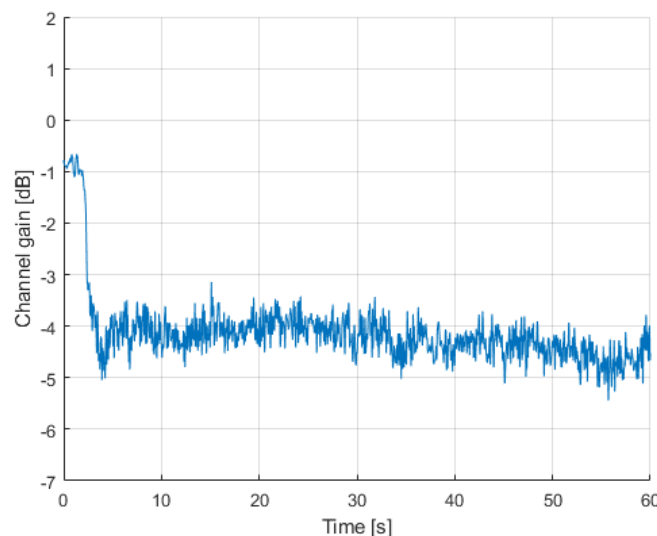


Figure 68: Channel gain over time, averaged over frequency, for 100 antennas in the distributed array when scanning the shadowed area on the left side of the corridor with a horizontal UE antenna

## 4.2 Millimeter-wave characteristics

Unfortunately, issues were discovered in the post-processing and hence it is not possible to present any channel characteristics from the mmWave measurements. The setup used is described in section 2.2 and is now working perfectly, however during the measurements, a still unknown error must have occurred. The sounder antennas have been verified and re-calibrated after the measurements in order to isolate, identify and correct the issue, but no workaround seems possible as the most likely explanation is that the transmitter and receiver switching schemes have lost synchronisation.

during measurements in a somewhat random order. The scenarios for analysis will still be outlined here for the interested reader.

#### 4.2.1 Scenario A: open corridor

The first scenario presented is scenario A, which includes an open corridor and is shown in Figure 6. The first experiment is seen in Figure 9 and includes one UE moving along the corridor, away from the BS. The BS is situated in one end of the corridor and next to the wall, see Figure 22. The vicinity of the BS is fairly open, in comparison to most locations in the factory, but there are metallic racks with boxes and people could pass by when performing their tasks. The view from the BS towards the UE is seen in Figure 69, which also gives an idea about the environment with a lot of metallic but also other materials that will cause reflections. The view of the UE towards the BS when the measurement started is seen in Figure 70.



Figure 69: View from the BS towards the corridor.



Figure 70: View from the first position of the UE towards the BS.

#### 4.2.2 Scenario B: semi-open environment with robot interaction

The second scenario presented is scenario B, which is a very dynamic semi-open environment, including a lot of robot interactions as well as interactions from humans. The scenario starts with the experiment shown in Figure 14 where the UE is moving away from the BS, stopping at discrete positions and doing a measurement where both the BS and the UE are static. As seen in the map in Figure 14, the BS is standing towards the wall; the view from the starting position towards the BS can be seen in Figure 71. To the left in the figure, a robot, which moves back and forth in the environment, can be seen and in the ceiling, there are tracks where material is transported. The side view of the UE in its starting position can be seen in Figure 72. At this starting position the distance between the UE and BS is 3.6 meters.

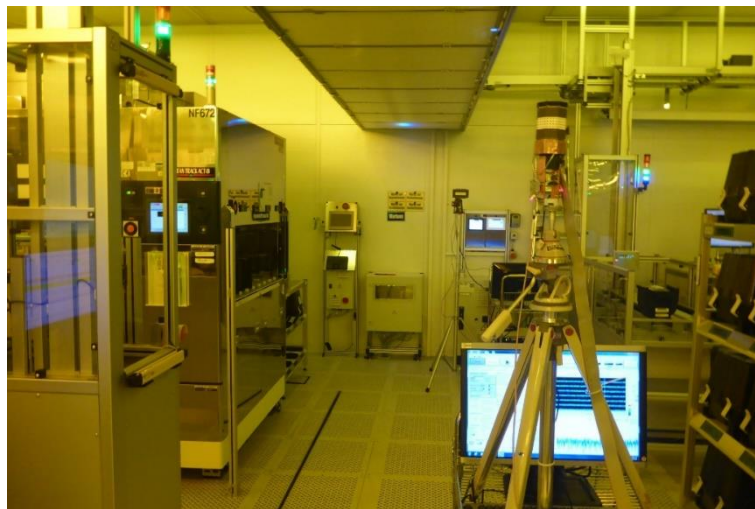


Figure 71: First UE position as seen from the UE towards the BS.

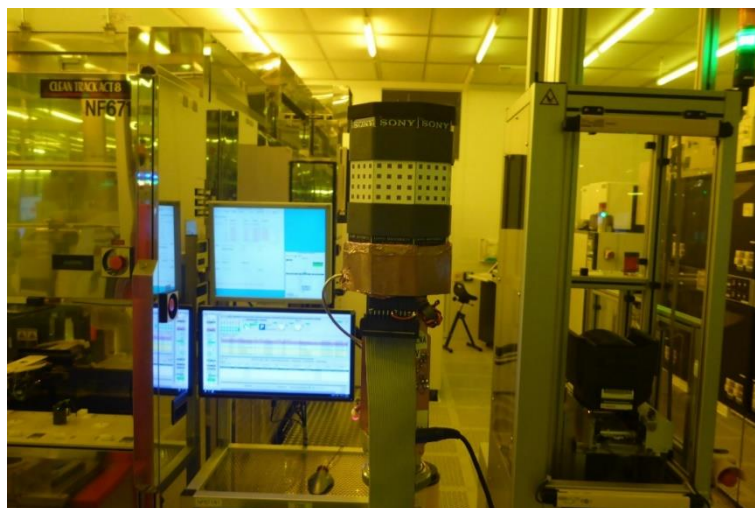


Figure 72: First UE position as seen from the side.

The same type of measurement was done at a second position along the route, 5 meters away from the first one. The view of the UE, facing the opposite direction of the BS, at this second position is seen in **Error! Reference source not found..**

The next analysed measurement as done with the mmWave equipment, is the experiment in Figure 15, which includes a LOS to NLOS transition. The UE starts in the middle of the corridor with LOS to the BS; the view from the UE to the BS is seen in Figure 73. Continuing on the path, the UE moves into a zone of obstructed LOS (OLOS), approximately seen in Figure 74. After that the UE continues in NLOS until the end of the corridor where the final position is seen in Figure 75.

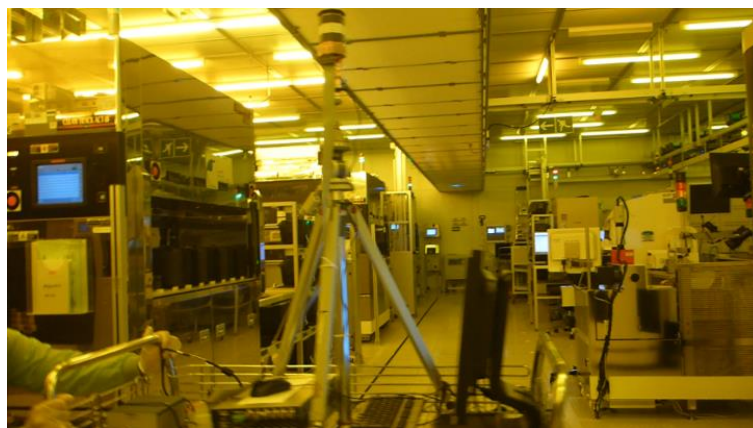


Figure 73: View from the UE towards the BS in the LOS case.

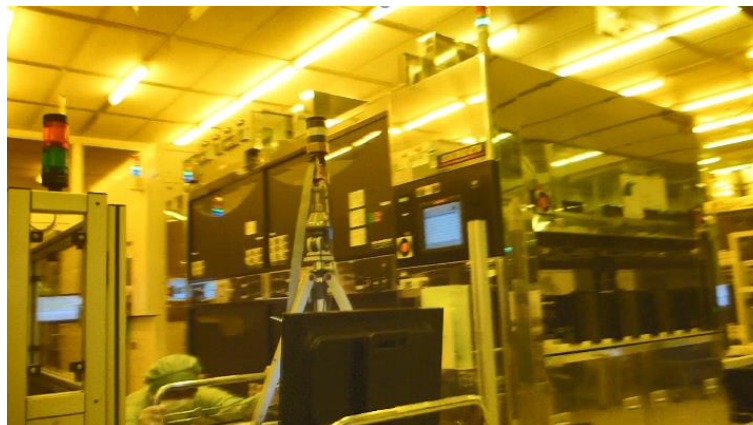


Figure 74: View from the UE towards the BS in the OLOS case.





Figure 75: View from the UE towards the BS in the NLOS case.

The last experiment for this scenario is the one that is also shown in Figure 14. Similarly as for the mid band measurements, the influence of robot interactions on the channel behaviour was captured. UE position A is shown in Figure 76, with the view from the UE towards the BS; at this point there are no robots nearby. At UE position B, two robots are in between the UE and BS – and one on the way – as seen in Figure 77. Lastly, at UE position C, two of the robots are out of the picture and only one is left, depicted in Figure 78.

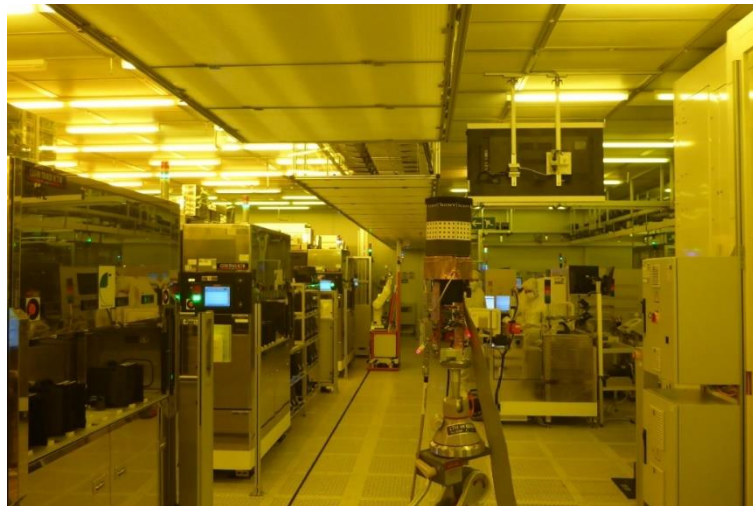


Figure 76: View from the UE towards the BS at UE position A.



Figure 77: View from the UE towards the BS at UE position B.

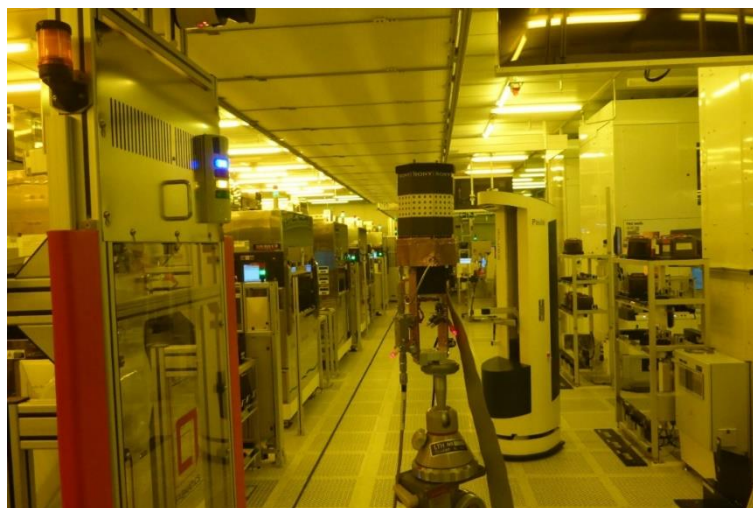


Figure 78: View from the UE towards the BS at UE position C.

#### 4.2.3 Scenario C: heavy blockage

The last scenario is scenario C that is a highly reflective environment with lots of high metallic equipment and narrow corridors. In general the environment is not a dynamic one, since there is no production in the area and for these measurements only the person moving the UE could have influenced the channel. In Figure 79Figure 38, the view from the BS towards the corridor when being empty is seen and in Figure 80 the same view can be seen but now including the UE. The first experiment in this scenario is the one seen in Figure 20, starting 3.2 meters from the BS and stopping 6 meters later. The side view of the UE at its starting position is seen in Figure 81 and the view towards the BS at the final position of the UE is seen in Figure 82.





Figure 79: View from the BS.



Figure 80: View towards the UE from the BS.



Figure 81: First UE position from the side.

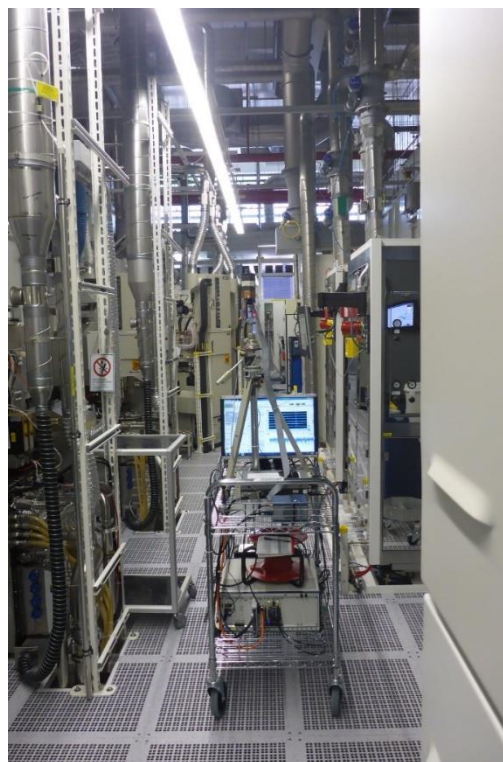


Figure 82: Last UE position with view towards the BS.

The last experiment presented is seen in Figure 21 and involves measurements of blockage profiles as the UE moves from NLOS to LOS and then back behind equipment again. The view towards the UE in its starting position is seen in Figure 83 and its final position in Figure 84.



Figure 83: View of the UE in the starting position in NLOS.



Figure 84: View of the UE in the final position in OLOS.



### 4.3 Summary of channel characteristics

To summarize some insights from the channel measurements, a massive MIMO system operating around 3.7 GHz shows promising characteristics in order to provide coverage over the factory floor. Even though there might be blocking due to walls, equipment, robots and humans, the blockage does not seem to be severe enough to hinder the deployment of a practical system in the environment. Comparing blockage due to NLOS transitions with blockage by robots, the first one in general provides a smoother transition while the latter often is more abrupt. Regarding robot interactions, the channel gain can also experience larger variations when there are robots in the near vicinity of the UE, acting as scatterers. Another observation is also the channel hardening effect that occurs when deploying a massive MIMO system. This effect results in a more stable channel in both time and frequency domain as the fading decreases as the number of antennas increases. This leads to reduced probability of outage and that smaller fading margins are required. On a final note regarding the mid band measurements, the results when deploying a centralised as well as a distributed array have been explored. From these initial results it is difficult to make any definite conclusions about differences as both show promising results and therefore further investigations are needed regarding their respective benefits and limitations.

Issues were identified in the post-processing in the data from the mmWave frequency band measurements and therefore no results can be presented. The performed experiments with related pictures are outlined.



## 5 Electromagnetic compatibility tests

The semiconductor testing at the Bosch plant in Reutlingen is performed at the test center, which is composed of two different production areas, the wafer test area in the second floor and the final test area in the first floor. These two areas also reflect the two types of tests, which are performed on the produced semiconductors.

The wafer test unit receives wafers directly from the different wafer fabs in Reutlingen and performs a fully automated electrical test under pre-defined conditions, e.g., operational temperature, for the semiconductor chips on the wafers. Figure 85 **Error! Reference source not found.** depicts an example of an 8-inch wafer, which undergoes the testing process. In addition to that, there are some additional process steps in the wafer level test, like the 100% automatic visual inspection of all tested wafers.

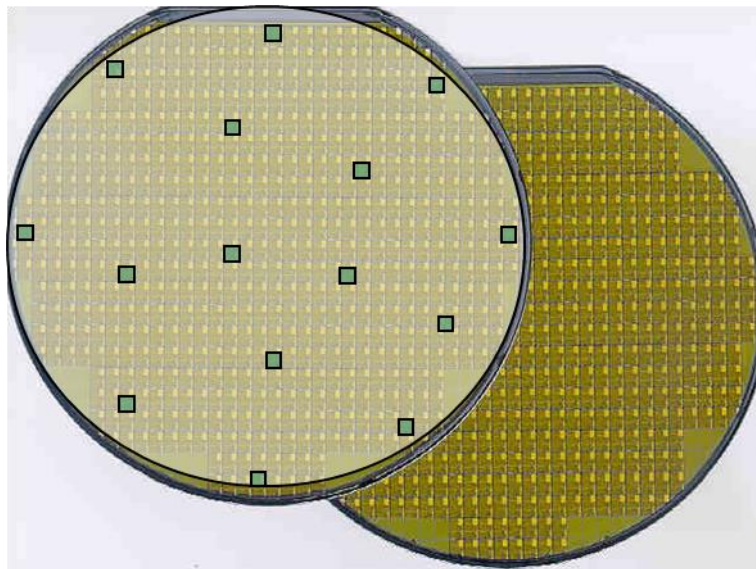


Figure 85: An 8-inch wafer (input to the wafer test)

The second type of test, i.e., the final test receives the semiconductor devices after assembly of the wafer chips into different packages, for examples see Figure 86. These tests perform different processes before the parts leave the factory and are delivered to customers. Main processes are the 100% electrical tests at -40°C for the automotive devices, i.e., devices used for the automotive industry. The semiconductor sensors, i.e. micro electro mechanical system (MEMS), are also tested with an additional physical stimuli. All devices are processed with 100% tape and real process before they are packed and delivered to customers.



Figure 86: Examples of semiconductor packages (input to final test unit)

Another area, where testing was conducted, is the sensor backend area. This area includes device assembly for special semiconductor packages and sensor test with physical stimuli, see Figure 87.

The different processes are carried out in several workshops. The sensor backend test receives wafers from the same locations as the test center.

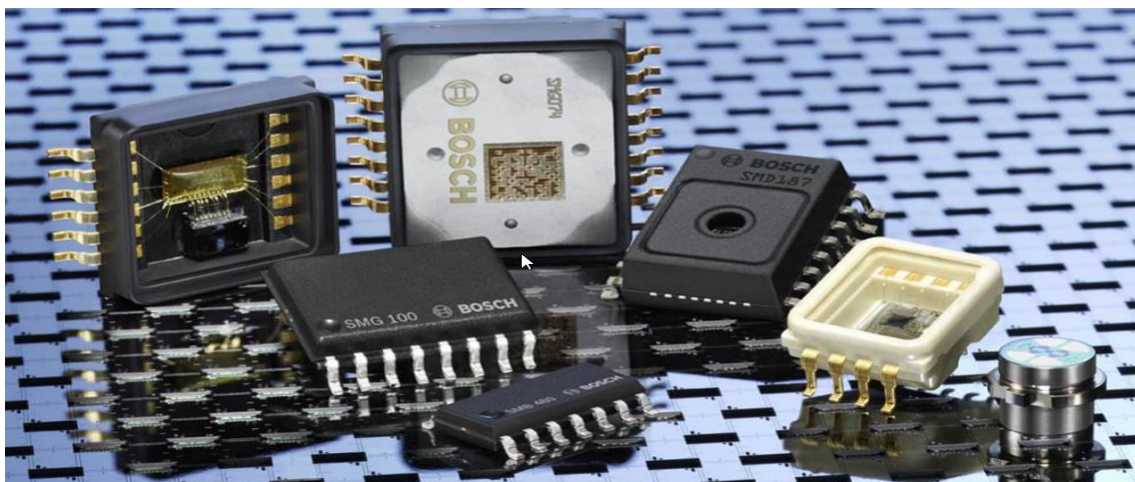


Figure 87: Different package types for devices in the sensor backend area

All test areas have controlled temperature and humidity conditions. The testing areas are clean rooms, which fulfill special requirements as defined according to various ISO classes. For the safety of the devices, all areas within the workshop are electro-static-discharge (ESD) protected areas (EPAs).





## 6 Device selection

Designing and conducting the EMC tests on the full range of active application specific integrated circuits (ASICs) and MEMSs produced in the factory is a very complicated task and goes beyond the scope of one research project. Therefore, the tests have been limited to a group of selected products. The products are carefully selected to have a representative result at the end. The EMC measurements are conducted in all the three test areas, i.e., wafer test, final test and sensor backend area, and cover testing of products belonging to both ASICs for automotive applications and MEMS. In particular, for the MEMS a mixture of products has been selected in order to cover different stimuli and test use cases. The MEMS are deployed in different automotive products, e.g., in electronic stability program, airbag controls and driver assistance, as well as in consumer products, e.g., in cell phones, tablets, environmental surveillance.

Table 3, Table 4 and Table 5 present all devices selected for the EMC measurements and corresponding description and test configurations. For all devices under test (DUTs), the measurement sequence as described later in the EMC test setup has been executed. Every different test system, handling/prober and DUT is indicated as a different Type in the tables below.

Table 3: Devices under test in wafer test area

Test system	Handling/Prober	Device under test	Device type
Type a	Type e	Type A	ASIC, mixed signal, monitoring transmission control
Type a	Type e	Type B	Acceleration MEMS for automotive
Type a	Type e	Type C	Inertial MEMS sensor for automotive
Type b	Type f	Type D	Smart power switch, ignition coil driver IC
Type c	Type g	Type E	Power MOS-FET for automotive
Type c	Type f	Type F	Control ASIC for NOX-System sensor, automotive
Type c	Type f	Type G	Evaluation circuit for yaw rate and acceleration sensor, automotive
Type c	Type f	Type H	Body sound evaluation circuit for acceleration sensor, automotive
Type d	Type e	Type I	Low-side switch for starter relays, automotive

Table 4: Devices under test in final test area

Test system	Handling/Prober	Device under test	Device type
Type a	Type i	Type J	Stabilised supply voltages, automotive
Type a	Type j	Type K	Inertial measurement unit, consumer
Type c	Type k	Type L	Acceleration sensor, consumer
Type c	Type j	Type M	Smart sensor, consumer

Type c	Type l	Type N	Current regulator, automotive
Type c	Type l	Type O	Engine management IC, automotive
Type c	Type l	Type P	Stabilized supply voltages, automotive
Type d	Type m	Type Q	Custom IC for evaluation of a plunger coil, digital, automotive
Type d	Type m	Type R	Double input amplifier for inductive sensors, automotive
Type h	Type n	Type S	Smart power switch, ignition coil driver IC

Table 5: Devices under test in sensor backend area

Test system	Handling/Prober	Device under test	Device type
Type o	Type o	Type T	Pressure sensor, automotive
Type p	Type p	Type U	Inertial measurement unit, automotive
Type y	Type y	Type V	Inertial measurement unit, automotive
Type x	Type x	Type W	Vehicle motion and position sensor, automotive

## 7 EMC test setup

Ericsson has developed the test setup to conduct the EMC test, which was shipped at Bosch Reutlingen site for the execution of the tests. It includes hardware and software as depicted in Figure 88.

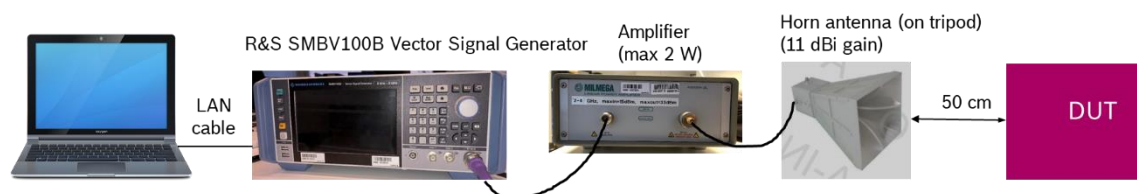


Figure 88. EMC Test Setup

The setup provides the uplink (UL) and downlink (DL) 5G new radio (NR) 3.7 GHz signal. The time-division duplex (TDD) is 75% for DL and 50% for UL.

The description of the UL and DL considered in the test cases are as follows:

- UL: 5G device at close proximity to the DUT (20cm) sending data to base station
- DL: 5G base station (Dot) installed in the ceiling approximately 2 meters away from the DUT

The horn antenna is located at 50cm distance from the device under test and for both DL and UL, the power level of the signal generator is adjusted to achieve the electrical field strengths due to the 5G signal at DUT for two operation scenarios: normal and worst. As a result, there are four operation scenarios: UL Normal, UL Worst, DL Normal, and DL Worst. The required peak values of the electric field strength for these different cases are summarized in Table 6.

Table 6: Required peak values of the electric field strength.

Operation scenario	Normal	Worst
UL	12.2 V/m	38.7 V/m
DL	5.5 V/m	10.9 V/m

The laptop has the drivers and the Matlab software needed for the vector signal generator to generate the necessary waveforms.

The Matlab program have an easy-to-use interface for doing the setup of the vector signal generator, which can be seen in Figure 89.

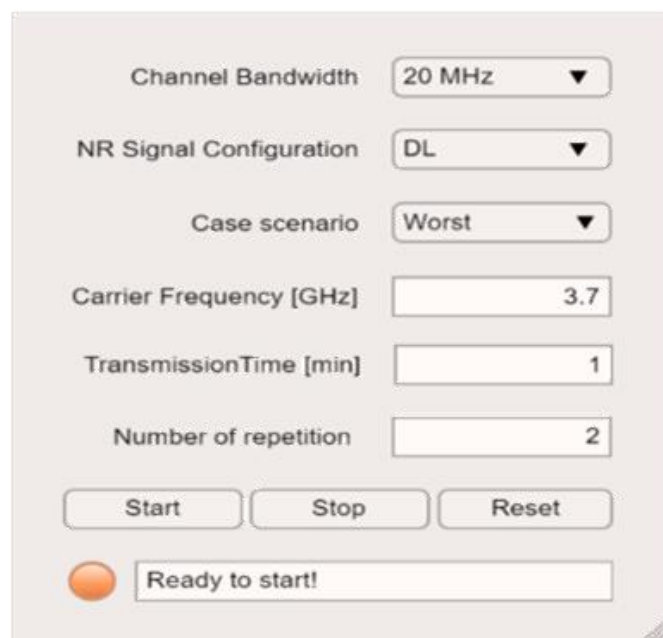


Figure 89: The interface for EMC testing

The configurations that are possible in the test setup are:

- Select a channel bandwidth of 20 MHz or 100 MHz
- Select signal configuration between UL and DL
- Select the operation scenario, worst or normal
- Select carrier frequency between 3.7 GHz and 3.8 GHz
- Transmission time (duration of the signal)
- Number of cycles (repetitions)

For the measurements on the shop floor, the carrier frequency was fixed at 3.7 GHz to reflect the actual deployment at the trial site. The duration of the signal was dependent from the test time of the DUT and the number of loops that the test program runs.

## 7.1 Test sequence and procedure

The test procedure always follows a given sequence, as depicted in Figure 90.

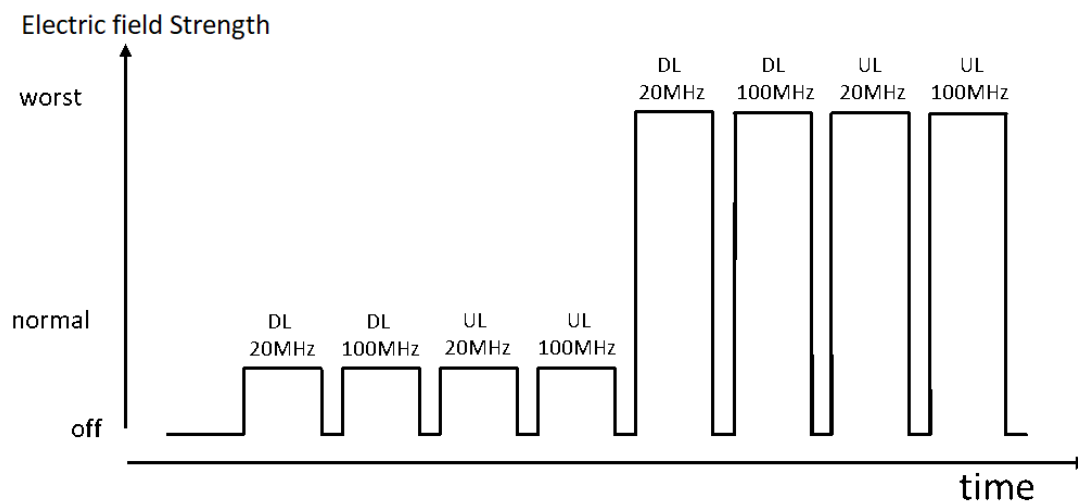


Figure 90: Test sequence

The loop count varies between 20 and 100 loops for the test program, run during the 5G signal duration. The loop count for the reference measurement also varies between 20 and 100 loops. The short measurement loops between the different 5G signals are for verification that the DUT is still working and not defect.

For the tests, EMC sensitive devices are chosen. The EMC test run with two different operation case scenarios, which are:

- Worst operation – with 50 cm distance to the antenna
- Normal operation – with 50 cm distance to the antenna

With different combinations of bandwidths and power levels, the functionality of the tested device without 5G signal is checked. All summed up, 17 runs per DUT with different loop counts per run was done.

## 7.2 Safety for series production

During the EMC tests the test cells are shielded with a special EMC suppressing foil as shown in Figure 91.

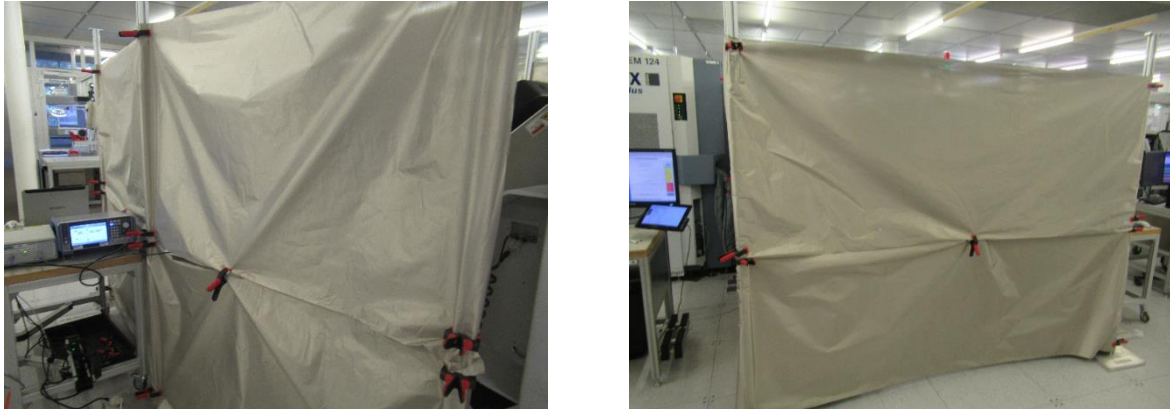


Figure 91: Shielding the test area for safety

With the setup, it is made sure that the direct environment in the workshop is not influenced. This helps preventing any interruption in the normal production during the 5G-SMART tests in the factory.

## 7.3 Analysis tool




The results were analysed with an internal data analysis tool, which is a universal post processing and analysis system for test data. A closer look into the repeatability and stability level (represented by the variable  $Cg^*$ , including drift/fails) of all measured values was made. With this parameter, the stability of the test hardware and test software was checked. It also has the capability to find out internal and external influence. Therefore, the  $Cg^*$  value was calculated for each test using the data analysis tool. The failed values for a given DUT was examined in detail to see if the 5G signals had any influence on the semiconductor test process.

## 8 EMC evaluation

Every failed test in the Cg\* analysis was checked for:

- Scatter within the test limits (which are product specific)
- Outliers
- Tests exceeding the test limits
- Site to site behavior, when a test program supports multisite testing (parallel testing of several devices with one test run)







































































































In the same checking procedure, it was checked if it occurs during the time when the 5G signal is or is not present. When the conspicuous data is within the 5G signal and it exceeds the test limits the test is marked as a fail. When the conspicuous data is within the 5G signal and it does not exceed the test limits, the test is marked as an outlier. All others are marked as passed and the colours representing these marks are as follows:

-  PASS
-  OUTLIER
-  FAIL

Test results for all devices are presented in Table 7, Table 8 and

Table 9.

Table 7: Test results for the wafer test area. N: Normal operation, W: Worst operation.

Test system	Wafer prober	Device under test (DUT)	5G off	DL 20 MHz N	5G off	DL 100 MHz N	5G off	UL 20 MHz N	5G off	UL 100 MHz N	5G off	DL 20 MHz W	5G off	DL 100 MHz W	5G off	UL 20 MHz W	5G off	UL 100 MHz W	5G off
Type a	Type e	Type A																	
Type a	Type e	Type B																	
Type a	Type e	Type C																	
Type b	Type f	Type D																	
Type c	Type g	Type E																	
Type c	Type f	Type F																	





Type c	Type f	Type G																	
Type c	Type f	Type H																	
Type d	Type e	Type I																	

Table 8: Test results in the final test area. N: Normal operation, W: Worst operation.

Test system	Handling/Prober	Device under test (DUT)	5G off	DL 20 MHz N	5G off	DL 100 MHz N	5G off	UL 20 MHz N	5G off	UL 100 MHz N	5G off	DL 20 MHz W	5G off	DL 100 MHz W	5G off	UL 20 MHz W	5G off	UL 100 MHz W	5G off
Type a	Type i	Type J																	
Type a	Type j	Type K																	
Type c	Type k	Type L																	
Type c	Type j	Type M																	
Type c	Type l	Type N																	
Type c	Type l	Type O																	
Type c	Type l	Type P																	
Type d	Type m	Type Q																	
Type d	Type m	Type R																	
Type h	Type n	Type S																	



Table 9: Test results in the sensor backend area. N: Normal operation, W: Worst operation.

Test system	Handling/Prober	Device under test (DUT)	5G off	DL 20 MHz N	5G off	DL 100 MHz N	5G off	UL 20 MHz N	5G off	UL 100 MHz N	5G off	DL 20 MHz W	5G off	DL 100 MHz W	5G off	UL 20 MHz W	5G off	UL 100 MHz W	5G off
Type o	Type o	Type T	●	●	●	●	●	●	●	●	●	●	●	●	●	●	●	●	●
Type p	Type p	Type U	●	●	●	●	●	●	●	●	●	●	●	●	●	●	●	●	●
Type y	Type y	Type V	●	●	●	●	●	●	●	●	●	●	●	●	●	●	●	●	●
Type x	Type x	Type W	●	●	●	●	●	●	●	●	●	●	●	●	●	●	●	●	●

As depicted in the tables above, the test result for all devices are marked as PASS, except for one device in the wafer test area. This indicates that the failed part Type H (body sound evaluation circuit for acceleration sensor, automotive) in the wafer test does not have the full EMC capability on wafer level. The full EMC capability is obtained after the assembly process of the semiconductor chip. After the assembly process the part will be tested on functionality again in the final test area before it gets delivered to a customer.



---

## 9 Conclusions and ways forward

In this report, the test setups and measurement campaigns performed in order to assess the possibility of deploying 5G systems in real operating factories in terms of coverage and EMC have been presented. Initial results have been presented to serve as a first assessment.

Regarding the channel measurements, operation of a massive MIMO system at 3.7 GHz shows promising characteristics in order to provide coverage over the factory floor. Both blocking profiles due to shadowing by walls and equipment as well as shadowing by humans and robots seems to be on such a level that it seems feasible that a practical system could provide coverage in the environment. Also, when combining the many antennas in a massive MIMO system, the fading decreases and as a result, a stable channel can be achieved in both time and frequency domain. Achieving this so-called channel hardening effect will improve the reliability of the communication in the environment. At this frequency, the characteristics both when deploying a centralised as well as a distributed array has been explored. Both show promising behaviour in the measured environment but further investigations are needed regarding their respective benefits and limitations.

When going up to the mmWave frequencies, the shadowing effects due to either walls and equipment or humans and robots were expected to become more severe. However, due to the rich scattering industrial environment, several MPCs were expected. However, due to the issues identified in the post-processing of the data, these two aspects could not be validated and characterised.

Future work regarding the channel measurements at mid band is to continue the evaluation of the already conducted measurement campaigns as well as to extract parameters in order to create and improve channel models that can be used to describe the factory environment. For the measurements at mmWave, the above aspects are planned to be analysed in a factory context in the future.

Based on the EMC test results, it can be concluded that with the actual tested samples, deploying a 5G network in

- the final test and the sensor backend areas can be considered without any concerns, and
- the wafer test area can not be considered unless actions are taken to ensure EMC.

It should be noted here that the above tests were conducted only on a subset of the active products in Bosch semiconductor factory in Reutlingen. That is, there may still be risks associated with EMC when deploying 5G in the final test and sensor backend areas. Accordingly, negative effects of 5G signals on untested devices, or in future test processes, can not be fully excluded.

As for the failed test, the following actions can be considered as a way forward:

- Run the 5G-SMART tests again on the Type H in wafer test and evaluate corrective actions.
- Check for solutions, like shielding between the pogo tower, test head and the wafer prober.
- If the additional action shows a positive result, then it needs to be discussed internally about a roll out of the solution in wafer test.
- Run, in defined periods, 5G EMC checks in the production area to see if new test technologies will be influenced.



---

Overall, this report can be concluded by the following. In terms of coverage in a factory, the 3.7 GHz channel measurements shows promising results. Regarding the EMC part, it can be concluded that the results look positive for a large number of devices but depending on the requirements of the specific production, compatibility may not be guaranteed for all. The results presented here are initial assessments regarding the deployability of 5G in real operating factories and further investigations are needed.



---

## 10 References

- [5GS20-D110] 5G-SMART, Deliverable 1.1, "Forward looking smart manufacturing use cases, requirements and KPIs", June 2020.
- [5GS20-D410] 5G-SMART, Deliverable 4.1, "Report on design and installation of the 5G trial system in Reutlingen", November 2020.
- [Ben19] E. L. Bengtsson, "Massive MIMO From a Terminal Perspective", PhD thesis, Department of Electrical and Information Technology, Lund University, 2019.
- [MVL+17] S. Malkowsky, J. Vieira, L. Liu, P. Harris, K. Nieman, N. Kundargi, I. C. Wong, F. Tufvesson, V. Öwall and O. Edfors, "The World's First Real-Time Testbed for Massive MIMO: Design, Implementation, and Validation," IEEE Access, vol. 5, pp. 9073-9088, 2017.
- [YZB+20] Z. Ying, K. Zhao, E.L. Bengtsson, H. Tataria, and F. Tufvesson, "Design of Switched Antenna Arrays for a 28 GHz Propagation Channel Sounder", in 2020 IEEE International Symposium on Antennas and Propagation and North American Radio Science Meeting: 2020 IEEE/URSI APS, 2020.



## Appendix

### List of abbreviations

Table 10: List of abbreviations

<b>AoA</b>	Angle-of-arrival
<b>ASIC</b>	Application specific integrated circuit
<b>BS</b>	Base station
<b>DL</b>	Downlink
<b>DUT</b>	Device under test
<b>EMC</b>	Electromagnetic compatibility
<b>ESD</b>	Electro-static-discharge
<b>EPA</b>	ESD protected area
<b>LOS</b>	Line of sight
<b>LTE</b>	Long-Term Evolution
<b>LuMaMi</b>	Lund university massive MIMO
<b>MEMS</b>	Micro electro mechanical system
<b>MIMO</b>	Multiple input multiple output
<b>mmWave</b>	Millimeter wave
<b>MPC</b>	Multipath component
<b>NLOS</b>	Non-line of sight
<b>NR</b>	New radio
<b>OFDM</b>	Orthogonal frequency-division multiplexing
<b>OLOS</b>	Obstructed Line of sight
<b>PDP</b>	Power delay profile
<b>RF</b>	Radio-frequency
<b>SDR</b>	Software-defined radio
<b>TDD</b>	Time-division duplex
<b>UE</b>	User equipment
<b>UL</b>	Uplink
<b>ZC</b>	Zadoff-Chu